THESIS FOR THE DEGREE OF DOCTOR OF PHILOSOPHY (PH.D.)

PHENOTYPIC PROFILE AND ROLE OF CANCER STEM CELLS IN UVEAL MELANOMA

Luna Djirackor M.D

Supervised by:

Prof. Dr. Goran Petrovski, MD, PhD, Dr. Habil.

Prof. Dr. Sarah Coupland, MBBS, PhD, FRCPath

Dr. Helen Kalirai, MSc, PhD

UNIVERSITY OF SZEGED

DOCTORAL SCHOOL OF CLINICAL MEDICINE

DEPARTMENT OF OPHTALMOLOGY

SZEGED, 2019

Scientific articles and publications

Publications related to the thesis

I. **Djirackor L,** Kalirai H, Coupland SE, Petrovski G.
CD166^{high} uveal melanoma cells represent a subpopulation with enhanced migratory capacity.
Invest Ophthalmol Vis Sci. 2019 Jun 3;60(7):2696-2704. doi: 10.1167/iovs.18-26431.
IF: 3.82

II. **Djirackor L**, Shakir D, Kalirai H, Petrovski G, Coupland S.
Nestin expression in primary and metastatic uveal melanoma– possible biomarker for high-risk uveal melanoma.
Acta Ophthalmol. 2018 Aug;96(5):503-509
IF: 3.03

Other Publications

III. Gáspár R, Pipicz M, Hawchar F, Kovács D, **Djirackor L**, Görbe A, Varga ZV, Kiricsi M, Petrovski G, Gácser A, Csonka C, Csont T.
The cytoprotective effect of biglycan core protein involves Toll-like receptor 4 signalling in cardiomyocytes.
J Mol Cell Cardiol. 2016 Oct; 99:138-150.
IF: 3.81

Impact factor of publications related to the thesis: 6.85
Impact factor of all publications: 10.66

Contents

List of Abbreviations

AACR- American Association for Cancer Research

AEC-3-amino-9-ethylcarbazole

AJCC- American Joint Committee on Cancer

ALCAM- Activated leukocyte cell adhesion molecule

BAP1- BRCA1 associated protein-1

BCA- bicinchoninic acid assay

BSA- Bovine serum albumin

CNVs- Copy number variations

CSCs- cancer stem cells

D3- Disomy 3

DAB- 3,3′-diaminobenzidine

DMEM- Dulbecco's Modified Eagle Medium

ECM- Extracellular matrix

EGF- Epidermal growth factor

EMT- epithelial-to-mesenchymal transition

EOE- extraocular extension

FACS- Fluorescence activated cell sorting

FCS- Fetal Calf serum

FFPE- formalin fixed paraffin embedded

GNA11- Guanine nucleotide-binding protein G(q) subunit alpha-11

GNAQ- Guanine nucleotide-binding protein G(q) subunit alpha

H&E -Haematoxylin and eosin

HR- High risk

HRP- Horseradish peroxidase

HSC- hematopoietic stem cell

HUVEC- Human Umbilical Vein Endothelial Cell

IF- Intermediate filament

IOP-intraocular pressure

LBD- largest basal diameter

LFTs- Liver function tests

LR- Low risk

M3- Monosomy 3

MAPK- Mitogen Activated protein kinases

MGM- Melanocyte Growth Media

MIA- Melanoma inhibitory activity

MITF- microphthalmia-associated transcription factor

MLPA- Multiplex ligation-dependent probe amplification

MRI- Magnetic resonance imaging

MSA- microsatellite analysis

MUM- Metastatic Uveal Melanoma

NC- neural crest

NCM- Normal Choroidal Melanocyte

NGFR- Nerve Growth Factor Receptor

NFM- Non-Fat Milk

OCT- optical coherence tomography

PAS- Period Acid Schiff

PBR- Proton beam radiotherapy

PBS- Phosphate-buffered saline

PFA- Paraformaldehyde

PUM- Primary Uveal Melanoma

RIPA- Radioimmunoprecipitation assay

RPE- retina pigment epithelium

RPMI- Roswell Park Memorial Institute media

SDS- Sodium Dodecyl Sulphate

STC- short term cultures

TCGA-The Cancer Genome Atlas

TICs- tumour initiating cells

TNM- Tumour, Node, Metastasis

ULA- Ultra low attachment

UM- Uveal melanoma

US- Ultrasound

UV- Ultraviolet

Summary

Uveal melanoma (UM) is the most common primary intraocular malignancy occurring in adults. Despite successful treatment of the primary tumour approximately 50% of patients develop liver metastases. Typically, liver metastases are detected 1-3 years after ocular treatment. Sometimes the metastasis appears 10 or even 20 years after primary tumour treatment. The reason for such latency is yet to be understood. One hypothesis is that a subset of stem-like cancer cells remain dormant and are reactivated after many years. They then proliferate and give rise to the bulk of the tumour. Cancer stem cells (CSCs) are cells with the capacity to divide asymmetrically to produce another CSC and a daughter cell that gives rise to the bulk of the tumour. In addition to the key properties of CSCs of self-renewal and differentiation, they also possess features that enable them to generate, maintain, enhance tumour growth and resist conventional therapy. These include expression of putative stem cell markers, activation of embryonic signalling pathways, anoikis resistance/anchorage independent growth, dye/drug efflux, and the ability to change their metabolic signature among others. The aims of this thesis were to identify CSCs in UM, particularly their phenotypic profile and role in this disease.

To this end, I examined the expression of CSC and adhesion markers in normal choroidal melanocytes (NCM), UM cell lines and in primary UM cells (PUM) grown in adherent and non-adherent culture conditions. Several CSC markers; CD166, Nestin and CD271 were upregulated in high metastatic risk PUM compared with low metastatic risk PUM and NCM. Cells surviving anoikis showed increased expression of these markers. A tumour migration assay showed that a $CD166^{high}$ subpopulation isolated from a UM cell line had higher migratory capacity compared to the $CD166^{low}$ population. The data generated in this section identified putative CSC markers in UM.

The results of this thesis also showed that neural crest (NC) developmental/embryonic markers are expressed in UM, suggesting that these primitive pathways may be reactivated in this tumour. Detailed investigations of Nestin, a neural stem cell marker in UM patient tissue showed that increased expression of Nestin significantly correlates with known poor prognostic factors, such as epithelioid cell morphology, high mitotic count, the presence of closed connective loops, monosomy 3 and polysomy 8q. Nestin is also expressed in metastatic UM (MUM), which together with previous studies showing Nestin expression in circulating tumour cells, suggests that Nestin may be used as a biomarker in high-risk UM patients for early detection of disseminated disease.

Introduction

1.1. Incidence

Uveal melanoma (UM) is a malignant tumour thought to arise from an uncontrolled division and proliferation of melanocytes within the uveal tract, comprising the iris, ciliary body and choroid. The uveal tract is the vascularised middle layer of the eye between the sclera and retina(1). Although a rare tumour, UM is the most common primary intraocular tumour in adults.

UM occurs in about 6-8 individuals per million each year (2). It accounts for about 5% of all melanomas in humans (3). Fair-skinned populations are more affected than others, especially those with blue or grey eyes and blonde or red hair with cutaneous freckles or nevi (4). UM is seen more commonly in older people with only 1% being reported in patients of 18 years and under (5). The incidence of UM rises with increasing age, with more than 20 cases per million per year being reported in individuals aged 70 years and above (2). Males and females are affected equally (3).

In this introduction, the anatomy, diagnosis, treatment and prognostication of UM as well as an overview of metastatic UM will be discussed. Further on, a brief outline of the development of melanocytes will be given as well as the concept of stem cells in normal tissue and cancer.

1.2. Anatomical and clinical features of UM

1.2.1. Choroidal Melanoma

The choroid is the largest part of the uvea, located in the posterior part of the eye. It is comprised of blood vessels, melanocytes, fibroblasts, resident immunocompetent cells and supporting collagenous and elastic connective tissue. Its functions include providing oxygen and nutrients to the outer retina, light absorption, thermoregulation, modulation of intraocular pressure (IOP) and drainage of aqueous humour (6). Ninety percent of UM arise from this region (**Fig. 1.1**.) (7). Choroidal melanomas may remain restricted by the Bruch's membrane and thereby have a "dome shaped" pattern resulting in small retinal detachment and deposition of lipofuscin in the subretinal space. If the tumour breaks through Bruch's membrane, it may appear as a "collar-stud" or "mushroom" shape and leads to subretinal exudation, and typically to a large retinal detachment. This is one of the pathognomonic clinical features of the disease (8).

1.2.2. Ciliary Body Melanoma

The ciliary body is an anterior extension of the choroid. It is made up of two structures: the ciliary muscle and the ciliary processes. The latter are ridge-like structures that increase the surface area for aqueous humour secretion. The ciliary muscle and ciliary processes make up the *pars plicata* (Latin: folded portion), which is the anterior portion of the ciliary body. The *pars plana* (Latin: flat portion) is the posterior area of the ciliary body: it has no known function after birth and is often used as an entry site during vitrectomy(1).

Five percent of UM develop in the ciliary body (**Fig. 1.1**) (7). Ciliary body melanomas tend to be diagnosed later than choroidal ones because they present with visual symptoms later and may be overlooked if dilation of the pupil is not undertaken during routine ophthalmological examinations. Presenting symptoms may include unilateral cataract, elevated IOP, and dilated episcleral vessels in the corresponding eye. Visual field defects do not occur until the tumour is large enough to cause obstruction of the pupil (9).

1.2.3 Iris melanoma

The iris is the diaphragm separating the anterior chamber from the posterior chamber. It is the anterior most part of the uvea and is in front of the lens. Its contraction and dilation, which is influenced by the sphincter and dilator muscles respectively, influence the amount of light entering the eye through the pupil. The iris also determines the eye colour due to the melanin in the posterior pigment epithelium (10).

Iris melanomas are often small nodular lesions that are deeply pigmented (**Fig. 1.1**). The anatomic location allows for earlier detection. Diffuse iris melanoma, which is a rare, more aggressive variant of the tumour may also occur. It typically causes glaucoma by obstructing the aqueous outflow pathway, including the trabecular meshwork and Schlemm's canal. Such iris melanomas have an increased risk of metastasis (9).

1.3 Diagnosis and Treatment

1.3.1. Signs, symptoms and diagnosis

Blurred vision, flashing lights or shadows, opaqueness of the lens, and glaucoma may be the first symptoms that patients experience. Upon visiting an optometrist or ophthalmologist, the diagnosis of UM would be made after a slit lamp, direct ophthalmoscope examination, ultrasonography or optical coherence tomography (OCT) (11). For many patients, the diagnosis is made during routine eye examination as the tumour may not present any

symptoms. Pain is experienced in <1% of cases and may be due to increased IOP from iris neovascularization or closed angle glaucoma. (12).

Characterisation of the tumour size is often performed by ultrasonography. Traditionally, this was based on the largest basal diameter (LBD). This classification has been updated in the 8th Tumour, Node and Metastasis (TNM) staging system, devised by the American Joint Committee on Cancer (AJCC), which is an anatomical staging system applied in all cancers (13). It enables the UM to be staged based not only by its LBD and thickness, but also by its extraocular extension (EOE) and/or ciliary body involvement (CBI) (14). Different examples of the shape, size and location of UM are shown in **Fig. 1.2**.

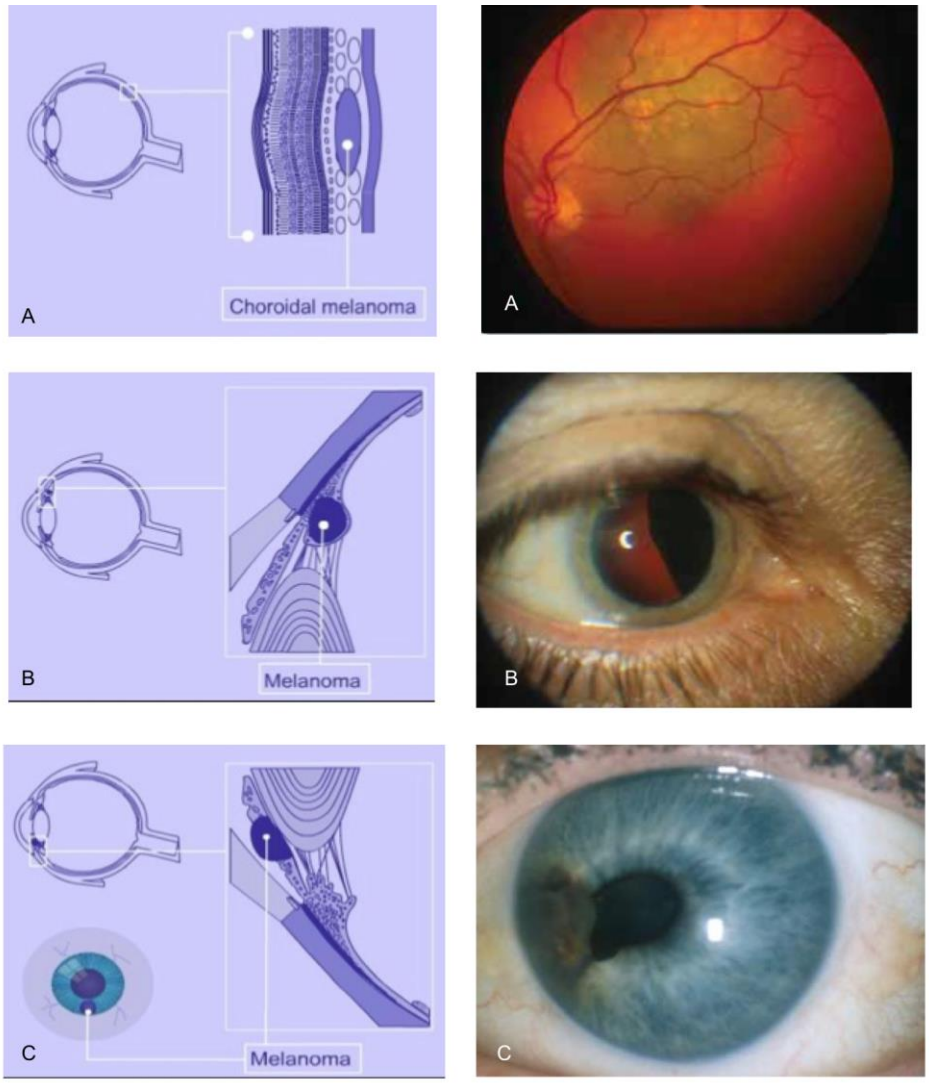

Figure 1.1 *Anatomical location and clinical appearance of UM.* ***A****) Choroidal melanoma;* ***B****) Ciliary body melanoma;* ***C****) Iris melanoma (Courtesy of Prof. B. Damato).*

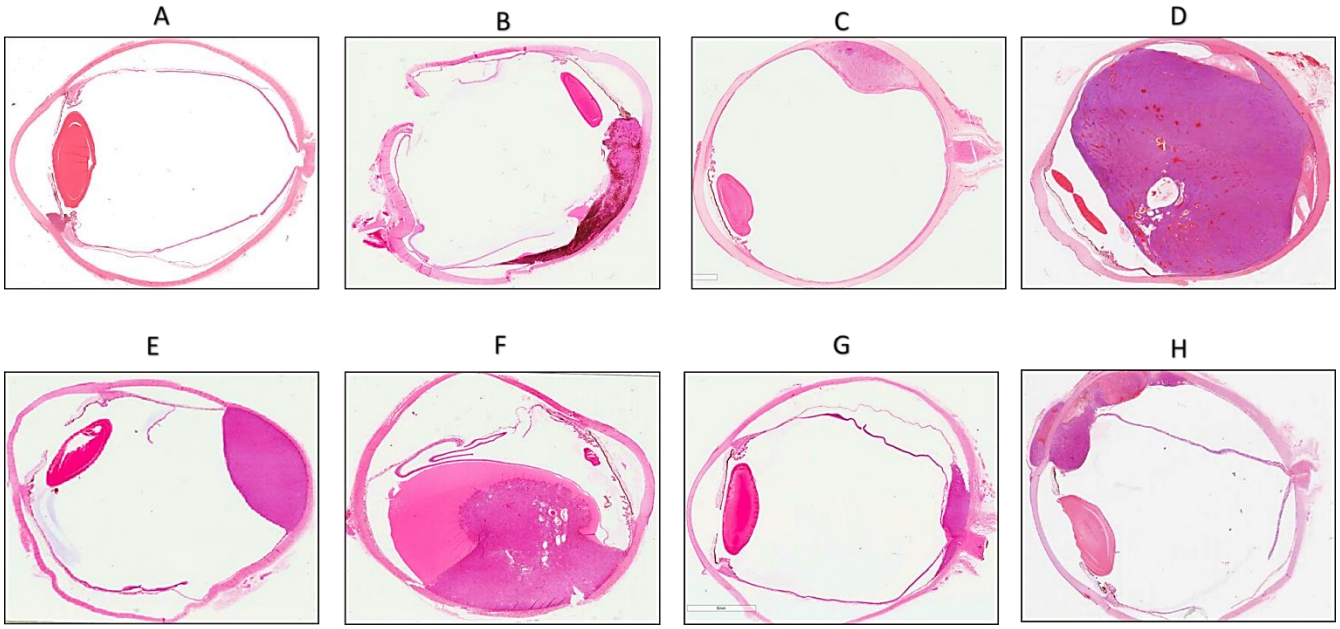

Figure 1.2 *H&E examples of the different sizes, shapes and locations of UM at 4x magnification.* ***(A)*** *Ciliary body melanoma,* ***(B)*** *Ciliochoroidal melanoma,* ***(C)*** *Choroidal melanoma,* ***(D)*** *Large choroidal melanoma,* ***(E)*** *Dome shaped choroidal melanoma,* ***(F)*** *Collar-stud choroidal melanoma,* ***(G)*** *Choroidal melanoma with optic nerve involvement,* ***(H)*** *Ciliochoroidal melanoma with extraocular extension (Courtesy of Prof. Coupland).*

1.3.2. Treatment

After the diagnosis of UM, management options are offered to the patient according to the tumour size and its location. Associated ocular co-morbidities and patient preference are other factors considered when determining UM treatment. Currently available treatment options include forms of radiotherapy, surgical excision, enucleation or phototherapy (reviewed by (15)).

Posterior UM are most commonly treated by radiotherapy. Brachytherapy using a radioactive plaque of Ruthenium-106 is most widely used in Europe, while the Iodine-125 isotope is the most popular in the USA (16). Tumour control is rated at 90% within 5 years using this treatment (17, 18). Side effects of radiotherapy including radiation retinopathy, exudative retinal detachment, neovascular glaucoma and radiation maculopathy may be experienced in some patients depending on radiation dose and isotope used(19, 20). This may lead to a secondary enucleation in 12-17% of cases (19).

Proton beam radiotherapy (PBR) is offered to patients in some specialised centres. It involves focusing a beam of radiation from an external source onto the tumour while sparing the surrounding tissue (21). It is modified to suit the tumour based on its size (between 2.5 and 10 mm in height and <16 mm basal diameter) (22) and location, and may be used for any UM, including iris melanomas (18). The region of radiation is marked by tantalum markers which are small inert metal buttons sutured to the sclera overlying the tumour. The patient is then placed in a fixed position, the eye is monitored with X-ray to visualise the markers and the radiation is administered (23). PBR is very effective in controlling UM; however, visual loss may occur, especially if the optic nerve or macula region are irradiated (24, 25).

Fractionated stereotactic radiotherapy is another treatment option that is widely available for the treatment of UM. It involves the use of a gamma knife, cyber knife or linear accelerator as the source of radiation. Doses of about 40 Gy in one fraction has been shown to result in acceptable local tumour control and low toxicity levels (26). The challenge of this treatment modality remains to be the high incidence of radiation-based complications, particularly neovascular glaucoma, resulting in secondary enucleation (27).

The two surgical techniques used to remove UM are called endoresection and 'exo' local resection. The former involves a pars plana vitrectomy after phacoemulsification with intraocular lens implantation. A 25-gauge cutter is used to cause posterior vitreous detachment and the choroidal tumour is 'hoovered' through the retina. Exoresection or local resection involves a partial lamellar sclera-uvectomy technique (28). To improve local control, adjuvant brachytherapy is commonly done after primary tumour resections (29).

Transpupillary thermotherapy and photodynamic therapy are two of the phototherapeutic treatment modalities available in UM management. Reviews show that the success of photodynamic therapy is higher in small, lightly pigmented or amelanotic choroidal melanomas and vascular tumours (30). Larger UM are not to be treated with this therapy (31). Transpupillary thermotherapy uses an infrared laser (810nm) which delivers heat at 45°-65°C, increasing the temperature of the tumour cells for about one minute. This disrupts their metabolic activity and coagulates the blood vessels (32). The efficacy of this treatment method has however been questioned as a study found that out of 391 patients, 42% of them had an intraocular recurrence. It is therefore recommended for only small choroidal melanomas with no more than two risk factors like lipofuscin, subretinal fluid, acoustic hollowness among others (33).

1.4. Prognostication

Approximately 50% of UM patients develop metastasis, most commonly to the liver. Personalised prognostication to determine metastatic risk, is available based on clinical, histopathological and genetic features of the tumour (34). This makes it possible to estimate the survival probability of an individual patient at the time of ocular treatment.

1.4.1. Clinical and histopathological features

The size of UM at the time of diagnosis influences prognosis because larger tumours have been known to be more aggressive (35). EOE, anterior location with CBI are predictors of a worse prognosis. These features are all included in the 'T' category of the TNM classification. In a study involving 7731 patients, results showed that the risk of metastasis and death increases two-fold with each increasing category from T1 to T4. The categories increase with increasing tumour base diameter and thickness. In addition, letters (a-d) are given depending on whether the tumour has CBI or EOE (36).

Histopathological analysis of formalin-fixed paraffin-embedded (FFPE) tumour sections after haematoxylin & eosin (H&E) staining also provides valuable prognostication data. The cell type of the melanoma cells whether epithelioid, spindle or mixed type based on the Callender classification is examined **(Fig.1.3)** (37). Epithelioid cells of polygonal shape, abundant cytoplasm, and poor cohesiveness are associated with a higher metastatic risk as compared to spindle cells, which are fusiform and in fascicles parallel to each other. Melanoma cells are part of a biological spectrum and histologic classification is subjective to some extent.

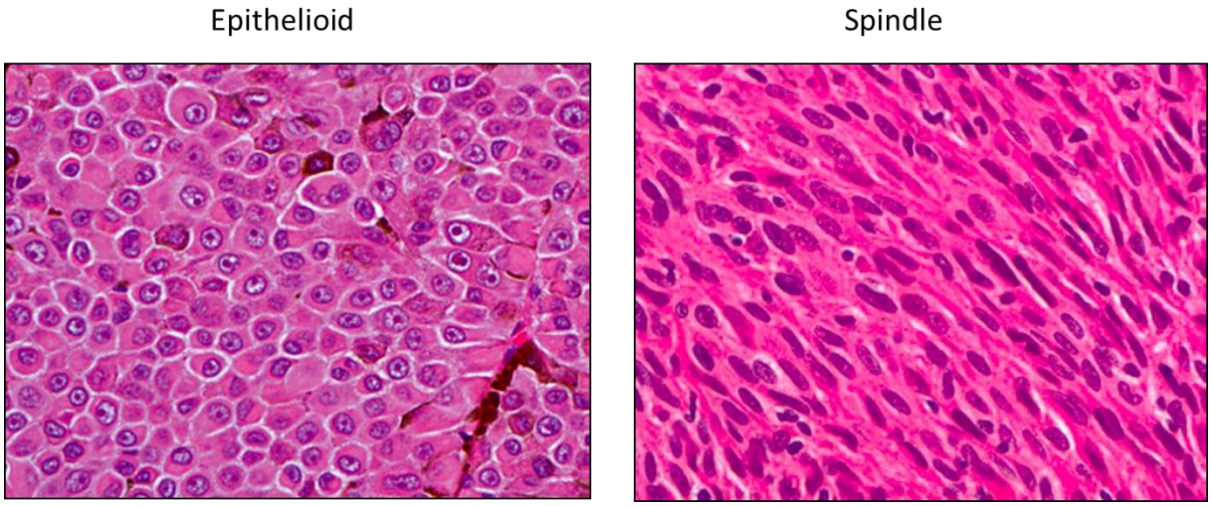

***Figure 1.3**. H&E stains showing epithelioid and spindle UM cells. (40x magnification) (Courtesy of Prof. Coupland).*

The mitotic count of the cells seen in H&E, together with the presence of closed connective tissue loops also determine the metastatic potential of UM (38). The mitotic count correlates with the proliferation rate of the tumour: the higher the number of mitotic figures, the worse the prognosis (38).

Increased metastatic risk is also associated with Period Acid Schiff (PAS) staining of the extracellular matrix of connective tissue closed loops. These 'loops' are a pattern of vasculogenic mimicry in the tumour (39). Other histopathological features of prognostic value include presence of tumour infiltrating lymphocytes, degree of pigmentation and presence/absence of necrosis (9).

1.4.2. Genetic profile.

1.4.2.1. Chromosomal aberrations

Copy number variations (CNVs) are seen in Chromosomes 1, 3, 6 and 8 in a large number of UM (40). These chromosomal aberrations can be used for prognostication. Several genetic analysis techniques have been used to detect CNVs. Patients seen at the Liverpool Ocular Oncology Centre are offered genetic testing of their UM, which is undertaken currently by multiplex-ligation-dependent amplification (MLPA) and microsatellite analysis (MSA). MLPA allows for relative quantification of multiple loci on chromosomes 1p, 3, 6 and 8 in a single reaction, increasing the cost effectiveness of the screening test. If the DNA from the sample is not sufficient for MLPA, MSA is performed to determine chromosome 3 status (40).

The loss of one copy of chromosome 3, i.e. monosomy 3 (M3), is the most important chromosomal abnormality in UM. It reduces the survival probability from 100% to less than 50% (41). The gain of the long arm of chromosome 8 (8q gain) is also associated with poor prognosis. A MLPA analysis of data from 452 UM patients undertaken by our group reported that M3 or 8q gain have a similar impact on survival when occurring alone (42). If a patient has both genetic alterations, the 5-year cumulative survival rate is reduced to 30% (43). The deletion of chromosome 1p is found in about 30% of UM (44). It shortens disease-free survival time if it occurs together with M3 (44). In contrast to the poor prognosis associated with chromosome 1p, 3 and 8 aberrations, polysomy 6p, (gain of 6p) is associated with prolonged survival and is commonly found in disomy 3 (D3) tumours.

1.4.2.2. Other genetic alterations

Unlike skin melanoma, UM has a low mutational burden and low levels of aneuploidy in the tumour cells. There is also no evidence of UV-light DNA damage in UM (45). The Mitogen Activated protein kinases (MAPK) pathway is activated in >80% of UMs by exclusive mutations in the G-coupled cell surface receptors: Guanine nucleotide-binding protein G(q) subunit alpha (GNAQ) or subunit alpha-11 (GNA11). These are gain-of function mutations that cause the MAPK pathway to be constitutively active (46).

The BRCA1-associated protein 1 (BAP1) plays a significant role in UM. The *BAP1* gene is located on chromosome 3 (3p21.31-p21.2) and encodes for a nuclear protein of the deubiquitinating enzyme family (47). This tumour suppressor protein is involved in several cellular processes including DNA repair, cell cycle regulation and protein trafficking. Dysregulation of these processes contributes to tumour development and progression (48). We have previously shown that loss of nuclear expression of BAP1 (nBAP1) in UM patients correlates with poor prognostic clinicopathological and genetic features and results in a reduced survival (49). In another study investigating the cellular expression of BAP1 and correlating it to prognosis, our group has shown that loss of nBAP1 expression is the strongest prognostic marker in UM (50). These data have been supported by findings from other studies including those by (51) (52) and the recent UM data from The Cancer Genome Atlas (TCGA) (53). IHC for nBAP1 expression is routinely performed at the Royal Liverpool Hospital NHS Trust to aid in UM prognostication.

1.5. Dissemination, detection and treatment of metastatic UM

Unfortunately, about 50% of UM patients develop metastasis despite successful treatment of the primary tumour. Metastatic spread is via the blood stream since the eye has no lymphatic drainage. Local dissemination of the tumour rarely occurs especially if the conjunctiva is intact and has not been infiltrated transclerally (54).

The liver is the main site for the metastatic dissemination of UM occurring in around 90% of cases. Other sites such as the lung, bone, skin occur occasionally but typically after liver metastasis (55). This observation led to the hypothesis that the liver provides a niche for the metastatic UM. Hence the former has been named the ’soil’ and the latter the ‘seed’ in Paget’s theory of metastasis, which was first described by Ernst Fuchs in 1882 (56).

Tumour doubling time and mathematical analysis suggests that metastatic spread occurs years before the primary UM is large enough to be detected clinically. Occult

micrometastases may be present in UM patients at the time of ocular treatment. Detectable metastatic tumours are present at the time of ocular diagnosis in only 1-2% of patients (57). Typically, liver metastases are detected 1-3 years after ocular treatment. Sometimes the metastasis appears 10, 20 even 40 years after primary tumour treatment. The reason for such latency is yet to be understood (58). Theories suggest that a subset of stem-like cancer cells remain dormant and are reactivated after many years. They then proliferate and give rise to the bulk of the tumour leading to a clinically detectable metastasis.

Once liver metastasis has developed, median survival time ranges from 2-12 months with 1-year survival being only 10-15% (59). Patients typically die from parenchymal invasion of the metastasis or from toxicity of the chemotherapeutic drugs. Recently, targeted systemic therapies, immunotherapies and local-regional treatments are being investigated for the treatment of metastatic UM. The best results regarding survival have been seen in patients with localised liver disease who are diagnosed early and undergo localised liver resection. Early detection of metastatic disease may aid in improving survival (9).

1.5.1 Screening tools for metastatic UM.

Ultrasound (US) and magnetic resonance imaging (MRI) are the most common imaging tools used for screening of metastatic UM. US has a high specificity but low sensitivity for the detection of metastatic lesions in the liver (60). It therefore needs to be supplemented with other tests if used for follow-up or screening. In Liverpool, the high risk (HR) UM patients are offered a liver MRI, which has enabled pre-symptomatic detection of liver disease in 92% of patients (61). There is a significant cost of MRI and it cannot be used as a life-long monitoring system for all UM patients. Liver function tests (LFTs) are also used to detect asymptomatic liver metastasis. The major disadvantage, however, is that the LFTs have a low specificity (27%) despite their high sensitivity (90-96%). This is because they are markers of liver damage, which may be caused by other substances such as cholesterol-lowering drugs or alcohol (62).

There is a need for more research to enable better understanding, monitoring and management of UM. One area that may benefit from more insight would be to identify the cell of origin of UM, and subsequently how tumourigenesis is initiated in these cells. There is no conclusive evidence to show where UM arises from. The most common theory is that UM arises from the malignant transformation of normal uveal melanocytes (63). Melanocytes differentiate from non-pigmented precursors called melanoblasts. These neural crest (NC)

derived melanoblasts migrate during embryogenesis from the neural plate border into the eye. Upon reaching the eye, the cells terminally differentiate to mature melanocytes and/or remain as immature melanocytic stem cells as evidenced in the skin (64). These primitive and migratory progenitor cells may undergo epigenetic and genetic changes to result in a malignant transformation. Alternatively, the mature and differentiated melanocytes may undergo dedifferentiation to become more 'stem-like', taking on the properties of their progenitor cells. Mutations in these cells may lead to cancer (65).

1.6. Developmental and migratory properties of melanocytes

The NC is a transient embryonic cell population that is from the ectodermal germ layer. The cells initially reside at the dorsal neural plate border during gastrulation. As neurulation begins, the neural plate begins to close in order to form the neural tube (66). The NC cells are elevated coming to eventually lie at the dorsal aspect of the neural folds. At this point, these cells express neural crest genes, namely *FOXD3* and *SOX10* marking their specificity as NC cells (66). After neural tube closure, the NC cells begin a process of epithelial-to-mesenchymal (EMT) transition and migrate to different locations in the developing embryo (66). The EMT process involves the loss of cell-cell adhesion, cytoplasmic remodelling and morphological changes that allow the NC cells to emigrate from the neuroepithelium. During migration, they acquire cell-surface receptors, metalloproteases and cell adhesion molecules that enable them to respond properly to cell–cell interactions and environmental cues in their migration path. Once the NC cells arrive at their destination, they self-aggregate and begin terminal differentiation (67). NC cells generate elements of the craniofacial skeleton, sensory and autonomic ganglia of the peripheral nervous system, and skin pigment cells. The specific cells include chondroblasts and osteoblasts, adipocytes, neurons and glial cells, cells of the adrenal medulla and melanocytes (66) (**Fig. 1.4**).

Melanocyte lineage specification from NC cells is governed mostly by the microphthalmia-associated transcription factor (*MITF*) (68). This has been supported by studies showing that mice lacking *MITF* do not form melanocytes and the same is true in fish [10]. *MITF* transcriptional targets include genes for melanosomes (melanin containing organelles), melanin synthesis pathway and survival genes such as *Bcl2* (69). Germline mutations of *MITF* in humans leads to Waardenburg syndrome or Tietz syndrome characterised by lack of pigmentation and deafness, due to defects in otic melanocytes (69). *PAX3* and *SOX10* act synergistically to activate *MITF* (70). These two transcription factors also specify glial cells.

The downregulation of FOXD3 and SOX2 is what specifies the melanocyte lineage in the bipotent melanoblast glial progenitor cells (68).

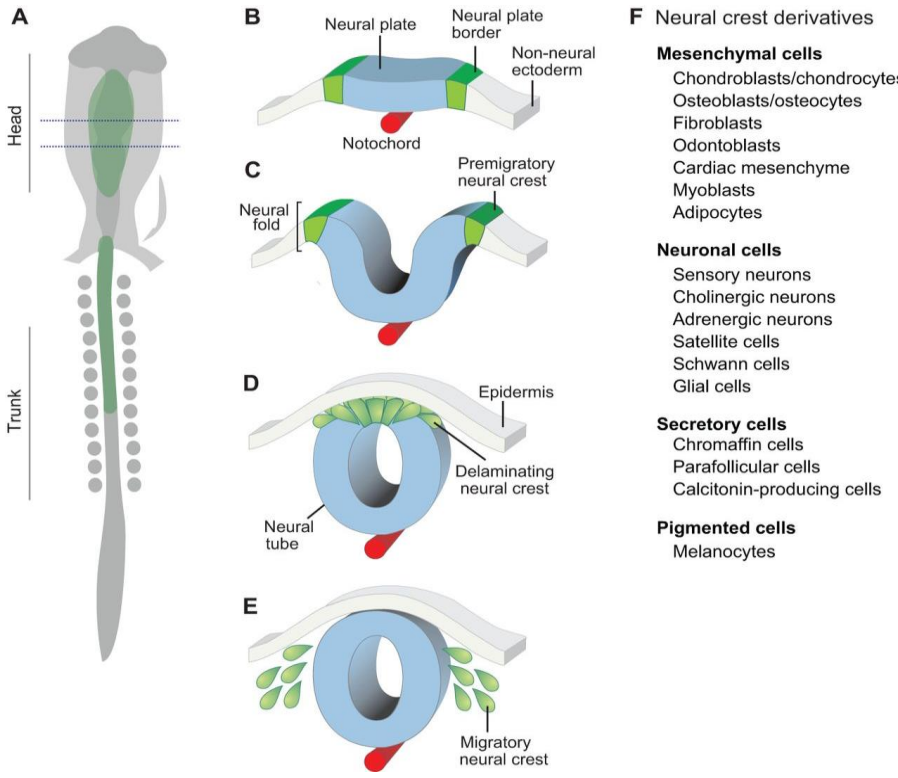

Figure 1.4 *Neural crest origin, migration and differentiation. Figure taken from Simoes-Costa, M. & M.E. Bronner, 2015(66).*

1.7. Stem cells in normal tissue and cancer.

The development of the embryo relies heavily on a group of cells with self-renewal and multi-lineage differentiation potential. These cells can undergo asymmetric cell division generating one daughter cell that retains the self-renewal and multi-lineage differentiation capacity while the other can become committed to a specific differentiation pathway (71). Stem cells in adult tissue also produce transient amplifying progenitor cells with the ability to undergo a limited number of cell divisions before finally differentiating terminally (71). The first evidence of stem cells was from the haematopoietic stem cells (HSC) (72). A single HSC was able to regenerate the blood system of a mouse. The transient amplifying progenitor cells, however, did not have self-renewal properties. When transplanted into an irradiated mouse, it could only produce cells for a short period of time (73).

There are striking similarities between normal organogenesis and carcinogenesis. Many of the oncogenes are known to promote self-renewal in normal stem cells and some tumour

suppressor genes also inhibit self-renewal in non-tumour tissue (74). Theories have therefore been proposed that cancer originates from deregulated stem cells or mature differentiated cells that have dedifferentiated and gained self-renewal properties. The consensus on which of these theories is correct is yet to be reached (reviewed by (75)). However, compelling evidence for the existence of stem cells in cancer has been provided. The American Association for Cancer Research (AACR) held a workshop to review this evidence, providing guidelines and defining several terms in this rapidly growing field. They gave the definition that cancer stem cells (CSCs) are cells with the capacity to divide asymmetrically to produce another CSC and a daughter cell that differentiates giving rise to the bulk of the tumour (76). CSCs may also be referred to as tumour initiating cells (TICs), describing their more functional role i.e. the capacity to form tumours when xenotransplanted (reviewed by (77))

In addition to the properties of self-renewal and differentiation, CSC/TIC also possess certain features that enable them to generate, maintain, enhance tumour growth and resist conventional therapy. These include expression of putative stem cell markers, activation of embryonic signalling pathways, anoikis resistance/anchorage independent growth, dye/drug efflux, EMT and the ability to change their metabolic signature among others (reviewed by (77)). Several of these properties have been used to identify and isolate CSCs in different cancers.

2. Aims of this study

1. To investigate the presence of CSC in UM by examination of several properties including the expression of putative stem cell markers, reactivation of developmental pathways and anoikis resistance.

2. To examine the expression of CSC- and adhesion markers in normal choroidal melanocytes (NCM), UM cell lines and in primary UM (PUM) cells grown in adherent and non-adherent culture conditions.

3. To examine if CSC markers influence patient outcome using the TCGA database.

4. To investigate the functional role of CSCs in UM cell lines.

5. To investigate if the developmental/stem cell markers that control cell proliferation and migration are expressed in UM tissue.

6. To investigate if the developmental/stem cell markers have an influence on UM prognostication and patient outcome by examining PUM and metastatic uveal melanoma (MUM) tissue.

3. Materials and Methods

3.1. Sample Collection

The globes of human cadavers were enucleated with consent at the Department of Pathology, University of Szeged and the Centre for Eye Research, University of Oslo, Norway. These eyes were used for cornea isolation and transplantation according to the ethically approved protocol of the Cornea and Tissue Bank in Oslo (REK ref.nr.:2017/418). After isolation of the cornea, normal choroidal melanocytes (NCM) were isolated and cultured, according to standard protocol that is described below under ‘’Cell culture’’.

Primary UM (PUM) samples were obtained from the Ocular Oncology Biobank (REC Ref 16/NW/0380) and Metastatic UM (MUM) samples were obtained from the Liverpool Bio-innovation Hub Biobank. They were used with patient consent and according to project specific ethical approvals from the Health Research Authority (REC Refs 11/NW/0759 and 15/SS/0097).

Human Umbilical Vein Endothelial Cells (HUVECs) were kindly donated by Professor Lu-Gang Yu of the University of Liverpool. This study was approved by the Health Research Authority and conducted in accordance with the Declaration of Helsinki.

3.2. Reagents

The reagents used for cell culture included products from Sigma-Aldrich (Dorset, UK): Penicillin/ Streptomycin, DMEM media, Dispase II, Glutamine, Collagenase IV, Collagenase I, Phosphate-Buffered Saline (PBS) and Bovine Serum Albumin (BSA). We obtained the following reagents from Life Technologies (Warrington, UK): Trypsin/EDTA, Roswell Park Memorial Institute (RPMI)-1640 media and non-enzymatic dissociation solution. The Fetal Calf Serum (FCS) was purchased from Labtech International Ltd (Heathfield, UK). For HUVEC cell culture, EGM-Plus media from Lonza (Slough, UK) was used. The NCM were cultured in melanocyte growth media (MGM) from Promocell (Heidelberg, Germany).

Additional reagents for flow cytometry included: paraformaldehyde (PFA) (Leica Microsystems, Milton Keynes, UK), Tween-20 (Fisher Scientific, Loughborough, UK) and normal goat serum (Vector Laboratories Ltd, Peterborough, UK). All the fluorescence-conjugated antibodies were from Biolegend (London, UK). The tissue culture treated flasks were from Thermo Scientific (Runcorn, UK) while the ultra-low attachment (ULA) flasks were purchased from Sigma (Dorset, UK). Flow cytometry readings were done on the FACS

Canto II cytometer from BD Bioscience. The FACS was done on the FACS Aria machine from the same company.

The CD166 and Nestin antibodies used for Western blot and IHC were purchased from Abcam (Cambridge, UK). All the reagents for the Western blot were from Biorad (Deeside, UK) except for the chemiluminescence reagents, which were from Thermo Scientific and the radioimmunoprecipitation assay (RIPA) buffer from Sigma. All the reagents for cell line IHC were from Dako, (Glostrup, Denmark) except the Vector AEC Substrate Kit from Vector Laboratories Ltd, Scott's tap water from Leica Microsystems and DPX mountant from Sigma. The human tissue IHC for CD166 was performed on the Bond RXm automated system from Leica Microsystems Ltd, (Milton Keynes, UK), which uses the Bond™ Polymer Refine Red Detection Kit. All the reagents and protocols for this were provided by the company. IHC for Nestin on PUM and MUM tissue was done using the Dako autostainer (Dako UK Ltd, Ely, Cambridgeshire, UK) which utilized reagents from the FLEX EnVision™ kit.

Tumour transendothelial migration assay was carried out on transwell plates from VWR International Ltd (Lutterworth, Leicestershire, UK).

3.3. Cell Culture.

The isolation of the NCM was done according to standard protocol, as previously reported (78). Briefly, after enucleation, the eye was put in a Petri-dish and washed with PBS+1% penicillin-streptomycin solution. A circumferential incision was made in the sclera, behind the limbus and the anterior segment, then the vitreous and sensory neuroretina were removed. Following this, trypsin was added inside the eye bulb and it was incubated at 37◦C for 1hr to remove the retinal pigment epithelial (RPE) cells. DMEM media was then used to flush the trypsin and the RPE were collected with gentle pipetting. The choroid was washed with the PBS-antibiotic mix. Following this, the choroid was then peeled from the sclera and placed in a petri dish. Subsequently, it was mechanically minced with a blade and re-suspended in a solution of 0.2U of Dispase. This was incubated for 18 hrs at 4°C with mild shaking, then at 37°C for 1hr. The wash medium was then added, and the supernatant collected and centrifuged. The pellet was then plated onto a 6-well plate in MGM.

Culture of PUM was performed as previously published (79). The piece of tumour tissue obtained from surgery was placed in a petri dish and cut to small pieces using a sterile blade. These tissue pieces were then re-suspended in collagenase I and incubated at 37°C for 1hr.

Enzyme activity was stopped by addition of media containing 1:1 αMEM: amnioselect, 10% FCS, 2 mM L-glutamine and antibiotics. The solution was centrifuged at 1500rpm for 2 mins. The supernatant was discarded and the cell pellet was re-suspended in fresh media and plated into a 25cm² flask. The media was changed every three days.

The UM cell lines, both PUM and metastatic UM (MUM), were maintained in RPMI media with 10% FCS, 2mM L-glutamine and penicillin-streptomycin. The cells were passaged once a week, and then used when they reached ~60% confluence. At the time of experimental analyses the cell lines were mycoplasma free and had STR profiles consistent with previously published data.

HUVEC cells were cultured in a specialised media called EGM from Lonza which contains growth factors and supplements such as bovine pituitary extract, hydrocortisone, epidermal growth factor (EGF) and antibiotics. The media was changed every three days, and when the cells formed a confluent monolayer, they were used for the experiments.

3.4. Flow cytometry

The NCM and the PUM cells were used for flow cytometry upon reaching ~60% confluency. They were detached using collagenase IV and a non-enzymatic dissociation solution, respectively. Following this, the blocking buffer (10% FCS, 0.02% EDTA in PBS) was added. The cells were centrifuged at 1500rpm for 2 mins and the supernatant removed. A flow cytometry buffer (PBS and 1% BSA) was added to the pellet and the cells were counted using a haemocytometer. 200,000 cells were then placed into each FACS tube in 100µl of flow cytometry buffer. The fluorescent antibody of interest was then added for the direct labelling of surface antigens. These included PE-conjugated anti-CD166, PE-conjugated anti-CD133 and FITC-conjugated anti-CD146. After 30 mins, the sample was washed with PBS and centrifuged. The remaining pellet was re-suspended in 500µl of flow cytometry buffer and run on the FACS Canto II cytometer.

Indirect labelling for the intracellular proteins involved cell fixation in 1% PFA for 10 mins. After washing with PBS, the cells were permeabilized with 0.5% Tween-20 solution for 10 mins. Blocking was performed using 10% normal goat serum in a 1% BSA and PBS solution. 10 mins later, the cells were washed with PBS and the primary antibody was added for 30 mins. The antibodies labelled indirectly were anti-Melan A, anti-CD271 and anti-Nestin. A wash was subsequently performed with PBS followed by a further 30 mins incubation at room temperature with a fluorescently conjugated secondary antibody (Goat Anti-Mouse IgG

H&L (Alexa Fluor 488) [ab150113]. After a final wash, the sample was re-suspended in 500µl of flow cytometry buffer and analysed on the FACS Canto II cytometer.

3.5. Adherent and non-adherent cultures for assessment of anoikis resistance

For the purpose of assessing possible changes in putative CSC marker expression during anoikis resistance in the UM cell lines, adherent and non-adherent cultures were employed. Briefly, cell lines that had been cultured to ~60% confluence were detached using the non-enzymatic dissociation solution. The cells were incubated in the solution for 5 mins at 37◦C followed by addition of an equal volume of RPMI culture media and centrifugation at 1500rpm for 2 mins. The cells were counted and $5x10^5$ cells were added to either a 75cm² tissue culture treated flask or a 75cm² ULA flask. An equal volume of media was added in both flasks. The cells were maintained in these conditions for 72 hrs, and subsequently labelled for flow cytometry according to the protocol detailed above.

3.6. Fluorescence activated cell sorting (FACS)

The Mel270 cell line was used for FACS sorting because it had two distinct subpopulations of $CD166^{high}$ and $CD166^{low}$ cells. The cell line was cultured in a 175cm² tissue culture flask until it reached ~60% confluence. The cells were dissociated using a non-enzymatic solution and counted. A total of 7 million cells were re-suspended in a FACS tube using FACS buffer (PBS, 1%BSA, 10%serum). Cells were labelled with the PE-conjugated CD166 antibody according to the protocol described under 'flow cytometry'. After 30 mins, the sample was washed with a PBS-based wash buffer and re-suspended in FACS buffer. Cell sorting was then performed after establishing the negative and positive gates using a PE-isotype control. The post-sorted cells were collected in media and plated into 25cm² flasks for 24hrs.

3.7. Tumour transendothelial migration assay

To mimic the process of extravasation across an endothelial cell layer into the blood stream a tumour transendothelial migration assay was performed as previously described (80). For this a 24-well plate with trans-well inserts having membranes with 0.8µm pores was used. Firstly, the HUVEC cells were harvested and counted. 30,000 cells were plated into each well insert and media changed daily for 3 days. When a confluent monolayer had been formed, the Mel270 cells were added. 40,000 cells of the Mel270 cell line were plated onto the HUVEC cell layer with media containing 1% FCS on the top while the in the bottom of the chamber the media contained 10% serum. This plate was incubated at 37°C for 48 hrs. Afterwards, the cell-dissociation and calcein-AM cocktail was added and after a 1hr incubation, the

fluorescence was measured at 485nm excitation and 520nm emission wavelengths in a GeNios Tecan plate reader (Tecan UK Ltd, Reading, UK).

3.8. Western Blotting

The specificity of the CD166 and Nestin antibodies used for immunohistochemistry was examined by Western blotting. Briefly, UM cell lines were grown to ~60% confluence in an adherent plate. Media was removed and the flask washed with cold PBS. RIPA buffer together with a protease cocktail inhibitor were added to the flask and a scraper was used to detach the cells. The suspension was then incubated on ice for 30 mins. Sonication was performed for 3 mins followed by heating at 95°C for 10 mins. After centrifugation at 14,000rpm, the supernatant was transferred to a new Eppendorf tube and stored at -20°C. The protein concentration was determined by a BCA assay (Biorad) according to manufacturer's instructions. 20µg of protein was loaded onto an SDS-PAGE gel and run for 2hrs, followed by transfer onto a nitrocellulose membrane of 0.45µm pore size. The membranes were blocked for 1 hr at room temperature in a solution of 5% non-fat milk (NFM) powder in 0.05% TBS-Tween20 (TBST). Overnight incubation in primary antibody (1:1000) diluted in 5% NFM powder was performed at 4°C. This was followed by three wash steps in TBST and a 1hr room temperature incubation with anti-rabbit horseradish peroxidase (HRP) conjugated secondary antibody (1:5000). After washing, the membranes were developed with an enhanced chemiluminescence kit according to manufacturer's guidelines. Imaging was undertaken on a GeneGnome XRQ Image capture machine.

3.9. Immunohistochemistry (IHC)

IHC for CD166 in the enucleated eye sections was performed on the automated Bond RXm System. The samples were prepared as 4 µm thick sections cut from FFPE tissue blocks. The kit used was the Bond™ Polymer Refine Red Detection, which applied a Fast-Red substrate chromogen. The slides were counterstained with haematoxylin and mounted using DPX mountant. Normal pancreas tissue sections were used as controls and positive staining in these demonstrated a valid IHC run. Slides were scanned using the Aperio CS2 Slide scanner from Leica and analysed with the Aperio Image Scope software version 11.2.

IHC staining for Nestin was performed on 4-µm-thick sections cut from FFPE tissue blocks. A Dako Pre-treatment module (Dako, Glostrup, Denmark) was used for dewaxing and heat-induced epitope retrieval. Slides were incubated in a high pH bath containing EnVision™ FLEX target retrieval solution (Tris/EDTA buffer pH9.0) at 96°C for 20 min, then stained

with a primary antibody on an autostainer (Dako UK Ltd, Ely, Cambridgeshire, UK) using the FLEX EnVision™ kit reagents. After being washed with FLEX wash buffer, samples were blocked with a FLEX peroxidase block for 5 min and incubated with a primary antibody for 30 min. Normal colon tissue sections listed in were used as controls and positive staining in these demonstrated a valid IHC run for Nestin.

IHC staining of UM cell lines grown on chamber slides was performed as follows: 0.2% Triton-X in PBS was added to each chamber for 5 mins to permeabilize the cells. After being washed with FLEX wash buffer, the samples were blocked with an EnVision™ FLEX peroxidase block for 5 mins and incubated with primary monoclonal antibody for 30 mins.

After being washed again, both the chamber slides and Nestin slides were incubated with a FLEX linker for 15 min. Bound antibody was then detected with horseradish peroxidase (HRP) for 20 min and visualized with an AEC Substrate Kit or DAB for 30 min. Sections were counterstained with Mayer's haematoxylin, blued with Scott's tap water and mounted with either Aquatex™ aqueous mountant (AEC) or DPX mountant (DAB). Omission of primary antibody was used as a negative control. Pictures were taken with the Nikon Eclipse Ci (Nikon UK Ltd, Surrey, UK).

3.10. IHC Scoring

IHC stained slides for all antibodies were scored by three independent observers. The percentage of positively-stained tumour cells was determined for all antibodies and this was used to grade the staining on a scale of 0-100%. In the Nestin stained slides, positive expression in the intratumoural capillary endothelium was also assessed, as either being present or absent.

3.11. Statistical analysis

Statistical analyses were undertaken for all the samples and markers. Categorical variables were tested using the Pearson's Chi-squared test and Fisher's exact test. A student t-test or Mann–Whitney test was used for to examine linear variables where the data did or did not fit a normal distribution respectively. To determine the threshold for Nestin positivity, a receiver operating curve (ROC) analysis was used. Difference in proportion for marker expression in the UM cell lines was assessed by z-statistics. Survival correlation was performed using the Kaplan– Meier test. A p-value <0.05 was considered to be statistically significant. All analyses were performed using SPSS software (ver.24.0; SPSS Science, Chicago, IL, USA).

4. Results

4.1. Cell culture of primary tissue.

The NCM were cultured until they reached 80% confluence and formed mature cells producing pigment. The cells were of spindle morphology with many melanosomes present in the cytoplasm. PUM cells showed both spindle and epithelioid morphology **(Fig.1.5).** There were varying amounts of melanin production in these cells consistent with histological sections of the primary tumour.

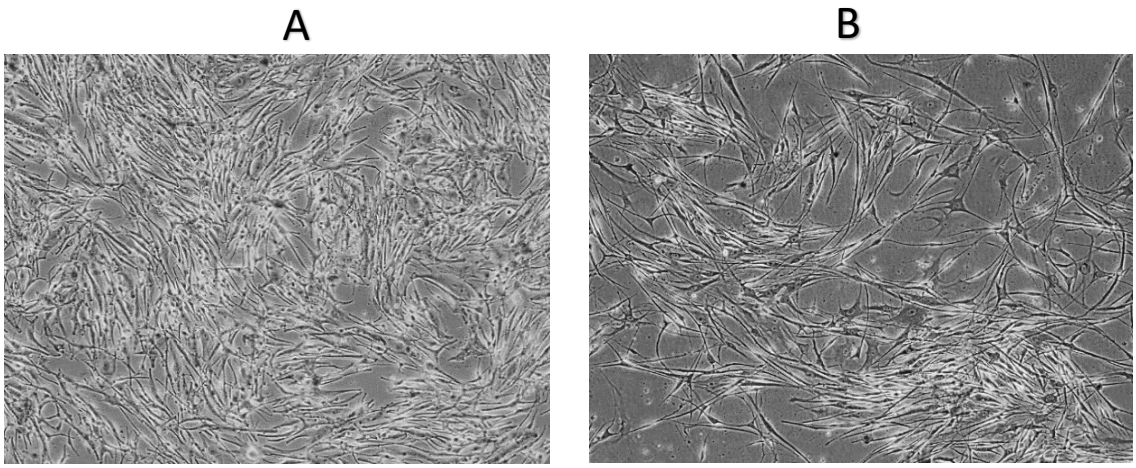

***Figure 1.5**. Representative images of NCM (**A**) and PUM tissue (**B**) at passage 0 in culture.*

4.2. CD166 and Nestin are upregulated in cultured PUM compared to NCM

When short term cultures (STC) of both NCM and PUM were investigated by flow cytometry, the stem cell markers CD166 and Nestin were found to be upregulated in PUM compared to NCM **(Fig. 1.6)**.

CD166 expression was 4-fold greater in the cultured PUM, (mean 78.3%, median 77.6%, range 54.1-99.6%) compared to its expression in the NCM, (mean 18.8%, median 15.5%, range 3.5-40.8%). This 4-fold increase in expression was found to be statistically significant **(p=0.0003**; Mann-Whitney). When correlated with chromosomal aberrations and histological prognostic factors, CD166 expression did not correlate with any known predictors of survival or disease outcome. Nestin expression was 1.6-fold higher in PUM (mean 33.1%, median 18.5%, range 0.04-99.3%) compared to NCM (mean 19.9%, median 16.5%, range 5.2-41.9%). However, this increased Nestin (p=0.12) together with the expression of Melan A(p=0.12), CD271 (p=0.14) CD146 (p=0.12) and CD133 (p=0.01) were not statistically

significant when a Mann-Whitney test was performed. Bonferroni corrections were made to the comparison between NCM and PUM ($p \leq 0.008$).

Of the ten PUM samples, five had features associated with a high metastatic risk (M3), four of these also having a loss of nBAP1 expression. When prognostic factors were correlated with the PUM results, they showed that M3 patients had a higher expression of CD271 (median 6.8%, range 0.5-30%) compared to D3 tumours (median 4.5%, range 0.2-22.2%). M3 patients also had a higher Nestin expression (median 19.8%, range 9.8-98.3%) than D3 patients (median 16.5%, range 0.04-99.3%). These changes were however not statistically significant when a Mann-Whitney test was performed CD271 ($p=0.42$) and Nestin ($p=1$).

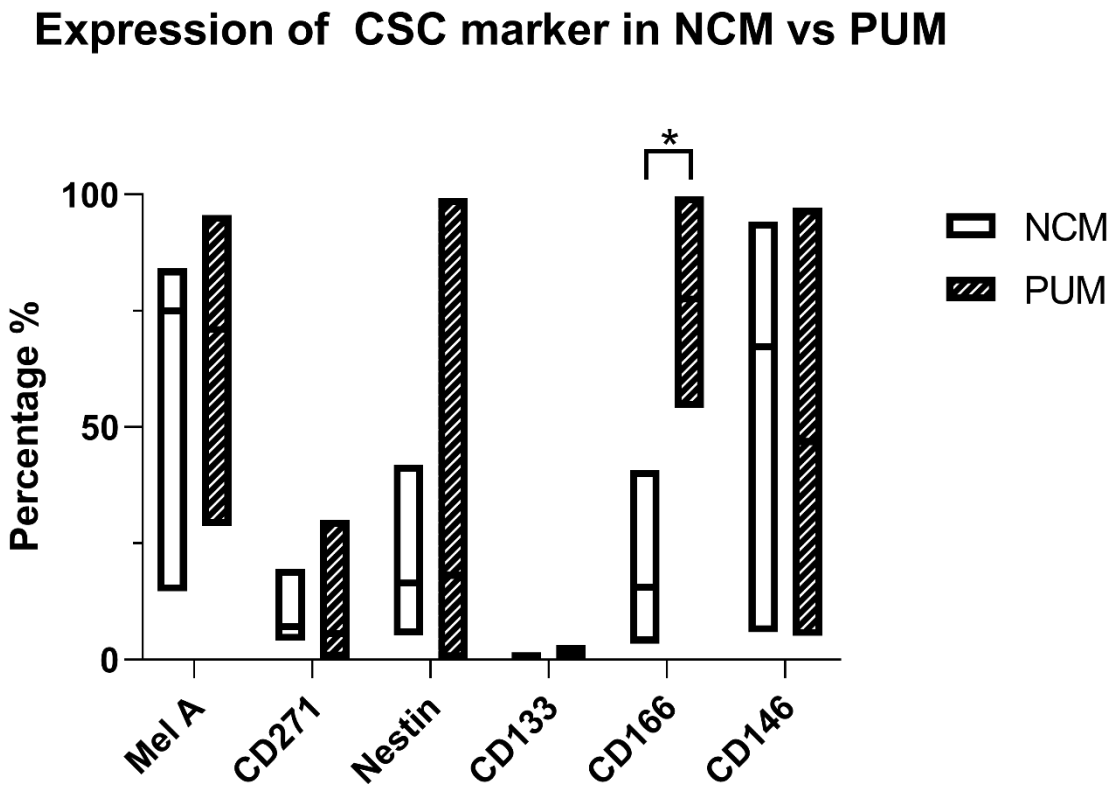

***Figure 1.6**. Graph showing expression of CSC markers in NCM(n=4) and PUM(n=10) cells. The bars represent the min-max percentage expression of the markers. The line is drawn at the median expression level of the markers. Statistically significant difference is shown with a star.*

4.3. CSC markers are upregulated in PUM cells during anoikis resistance.

Culturing cells in non-adherent/ultra-low attachment (ULA) conditions for 72 hrs ensured that only UM cells that were able to survive anoikis were viable. Comparison of the expression of CSC markers was made between the cells surviving anoikis/anchorage independent conditions and those grown in adherent monolayers. The UM cell lines used were derived from either PUM (92.1, Mel 270, MP41, MP46) or MUM (OMM1, OMM2.3, OMM2.5, MM66) samples. All the experiments were repeated at least 3 times and an average ± standard deviation (SD) was calculated. This is summarised in **Fig. 1.7** and **Table 1.1** below.

Melan A, the marker of differentiated melanocytes was expressed in at least 50% of all the cells in both adherent and non-adherent conditions (median 73.3% vs 71.8%).

CD271, the neural crest stem cell marker was expressed at low levels (median 1.0%, range 0.03-33.3%) in the cells grown as adherent cultures. The cells surviving anoikis, however, had a higher expression of this marker (median 8.9%, range 0.04-18.2%). These changes were statistically significant (**$p<0.01$**, z-statistic) in MP46, OMM1, and MM66. These data are represented in **Fig. 1.7** and **Table 1.1**.

Nestin, a neural stem cell marker of prognostic significance in both skin and uveal melanoma (81, 82) was upregulated in all cell lines after anchorage independent growth. During adherent culture, the median expression of Nestin was 25.5% (range 3.0-80.4%). After non-adherent culture, the cells had a median expression of 64.1% (range 19.8-97.5). Although this upregulation of Nestin expression was observed in 7/8 of the cell lines examined, these changes were statistically significant (**$p<0.01$**, z-statistic) only in 92.1, MP41, MP46, OMM2.3 and OMM 2.5.

CD133 is a stem cell marker in hepatocellular carcinoma, colorectal cancer and glioblastoma (83-85). Its expression was unchanged in both culture conditions, adherent (median 0.3%, range 0.1-0.6%) and non-adherent (median 0.4%, range 0.2-0.8%).

CD146 (MUC18 or MCAM) is a protein of the immunoglobulin family. It strongly expressed in metastatic skin melanoma cells (86) for the purpose of interacting with vascular tissue during haematogenous spread (87). The expression of CD146 was present in >70% of the UM cells and showed little change in either of the culture conditions.

CD166 is also a member of the immunoglobulin superfamily. It functions as a cell surface sensor for cell density, controlling the transition between local cell proliferation and tissue invasion in melanoma progression (88). Its expression was variable in the UM cell lines examined in adherent culture (median 34.8%, range 2.5-87.7%) and in non-adherent culture (median 30.5%, range 2.2-95.1%). Three of the four MUM cell lines [OMM1 (87.7-95.1%), OMM2.3 (3.7-6.9%), OMM2.5 (17.7-26.4%)] and one PUM; MP41 (3.1-18.0%) however, upregulated their expression of CD166 during anoikis resistance as compared with cells in adherent culture. Analyses by z-statistics showed that these changes were statistically significant MP41 (**p<0.01**) but not OMM1 (p=0.07), OMM2.3(p=0.35), or OMM2.5 (p=0.17).

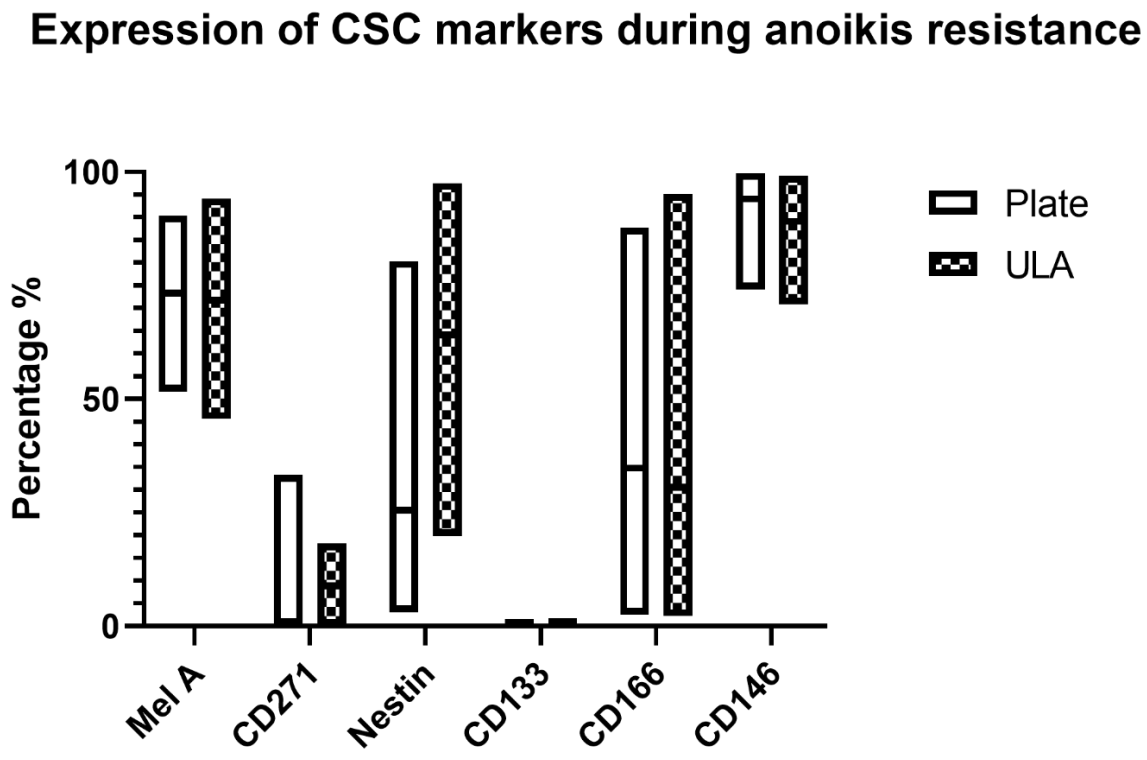

Figure 1.7*. Expression of CSC markers in UM cell lines cultured in adherent (plate) and non-adherent (ULA) conditions. The bars represent the min-max percentage expression of the markers. The line is drawn at the median expression level of the markers (n=3).*

***Table 1.1**. Expression of CSC markers in UM cell lines grown in adherent (plate) and non-adherent/ultra-low attachment (ULA) cultures. Numbers show mean percent (%) ± (SD) expression of protein markers. MUM cell lines are represented in **bold**. (*) samples from one experiment.*

UM cell line	Mel A	CD271	Nestin	CD133	CD166	CD146
92.1 plate	51.6 (2.8)	6.0 (0.1)	37.2 (3.2)	0.2 (0.2)	66.0 (32.7)	98.8 (0.6)
92.1 ULA	69.9 (2.7)	12.5 (9.7)	61.7 (1.9)	0.3 (0.2)	34.6 (31.2)	89.2 (13.4)
Mel 270 plate	59.4 (5.5)	0.9 (0.8)	17.6*	0.3 (0.01)	51.9 (18.1)	94.0 (8.3)
MEL 270 ULA	67.0 (10.2)	5.3 (3.9)	19.8 (9.2)	0.5 (0.5)	54.1 (20.9)	78.0 (29.4)
MP41 plate	71.3 (8.8)	1.2 (1.2)	8.1*	0.06 (0.08)	3.1 (3.9)	91.4 (17.3)
MP41 ULA	45.6 (9.5)	0.2 (0.3)	27.4*	0.3 (0.3)	18.2 (15.6)	98.3 (2.3)
MP46 plate	90.4 (1.5)	0.5 (0.1)	80.4*	0.5 (0.04)	51.8 (9.8)	74.1 (9.8)
MP46 ULA	94.2 (1.9)	16.3 (12)	97.5*	0.5 (0.1)	37.5 (21.0)	70.8 (6.2)
OMM1 plate	**62.2 (1.6)**	**33.3 (6.5)**	**33.5 (16)**	**0.6 (0.6)**	**87.7 (24.5)**	**93.4 (14.1)**
OMM1 ULA	**73.7 (0.7)**	**16.1 (1.9)**	**27.8 (25)**	**0.4 (0.5)**	**95.1 (3.0)**	**98.1 (1.8)**
Omm2.3 plate	**80.6 (21.8)**	**0.3 (0.4)**	**3.1***	**0.3 (0.2)**	**3.7 (2.6)**	**99.7 (0.4)**
Omm2.3 ULA	**86.1 (7.9)**	**0.04 (0.05)**	**86.6***	**0.2 (0.2)**	**6.9 (9.8)**	**87.3 (21.2)**
Omm2.5 plate	**80.5 (21.9)**	**0.5 (0.5)**	**5.9***	**0.2 (0.6)**	**17.7 (12.4)**	**94.1 (6.1)**
Omm2.5 ULA	**85.0 (11.9)**	**0.1 (0.2)**	**66.5***	**0.8 (0.1)**	**26.4 (25.7)**	**89.1 (12.3)**
MM66 plate	**75.3 (13.4)**	**1.5 (0.2)**	**75.9***	**0.4 (0.1)**	**2.5 (0.6)**	**99.7 (0.2)**
MM66 ULA	**75.3 (10.9)**	**18.2 (15.1)**	**81.2***	**0.3 (0.1)**	**2.2 (1.2)**	**99.1 (1.1)**

4.4. Nestin, CD271 and CD166 gene expression in 80 PUM analysed by TCGA.

The role of *Nestin*, *CD271* and *CD166/ALCAM* gene expression in UM and their correlation to other prognostic factors were investigated. This was undertaken by analysing the recently-published and publicly available data from The Cancer Genome Atlas (TCGA) for UM. It contains the genetic data of 80 well characterised PUM patients followed up for 5 years (53). mRNA expression data was obtained from the database and compared with chromosome 3 CNVs, BAP1 gene expression and patient outcome. Analysis was done using Xena Browser (https://xenabrowser.net/heatmap/) and the results displayed using Corel Draw graphics software.

Median expression levels of the genes (white colour) were used as the cut off points and upregulation was displayed in red while downregulation was displayed in blue in the heat maps (**Fig. 1.8**). The median expression levels (unit log2(fpkm-uq+1)) of the genes were: *BAP1*(19.50), *ALCAM* (14.22), *Nestin* (19.02) and *CD271/NGRF* (13.2). Results showed that UM with M3 (i.e. associated with a poor prognosis) and decreased *BAP1* gene expression

compared to the median also had upregulations in *CD166/ALCAM* expression. The expression of *Nestin* and *CD271/NGRF* was more variable across the 80 samples with upregulations and downregulations occurring in the M3 as well as the D3 group in no distinct pattern. This is shown in the heat map of **Fig.1.8** below.

The Kaplan-Meier plots were created using the median expression levels as the cut off and statistics analysed by Chi-square test ($\chi 2$). The survival probability was calculated based on event (metastatic death) and time to event (number of days) as parameters. They show that UM expressing *CD166/ALCAM* above the median were associated with a poorer prognosis than those with expression below the median (**p=0.00321**). The expression of Nestin (p=0.31) and CD271/NGRF (p=0.68) had no statistically significant correlation with patient survival. *CD166/ALCAM* association with survival may not be as a result of its covariation with tumour stages (**Fig. 1.9**). Based on data from both the flow cytometry analyses and gene expression data, the functional role of CD166/ALCAM was investigated further.

4.5. Western blotting

In order to perform functional studies in UM cell lines, we purchased a CD166 antibody (Abcam: ab109215) that was not fluorescently-conjugated. The antibody was tested for antigen specificity by Western blot. The cell lysate of UM cell line Mel270 was run on an SDS-PAGE gel to determine CD166 protein expression. The cell line expressed CD166, visible as a band at the predicted molecular weight (100-105kDa) (**Fig. 1.10).** The antibody was specific for only this protein.

4.6. CD166 protein is expressed in the cytoplasm of PUM cell lines by IHC.

The expression pattern and cellular location of CD166 protein was examined in UM by IHC. Three cell lines (92.1, Mel270, OMM1) were cultured in chamber slides and stained by IHC for CD166. The UM cells 92.1 expressed CD166 in the cytoplasm of ~60% of the cells**.** The Mel270 cell line also showed cytoplasmic CD166 expression in approximately 40% of the cells (**Fig. 1.10).** OMM1 cells expressed CD166 only on the membrane. This expression was in at least 80% of the cells. Both cytoplasmic and membrane staining for CD166 has previously been reported in skin melanoma (89).

(I)

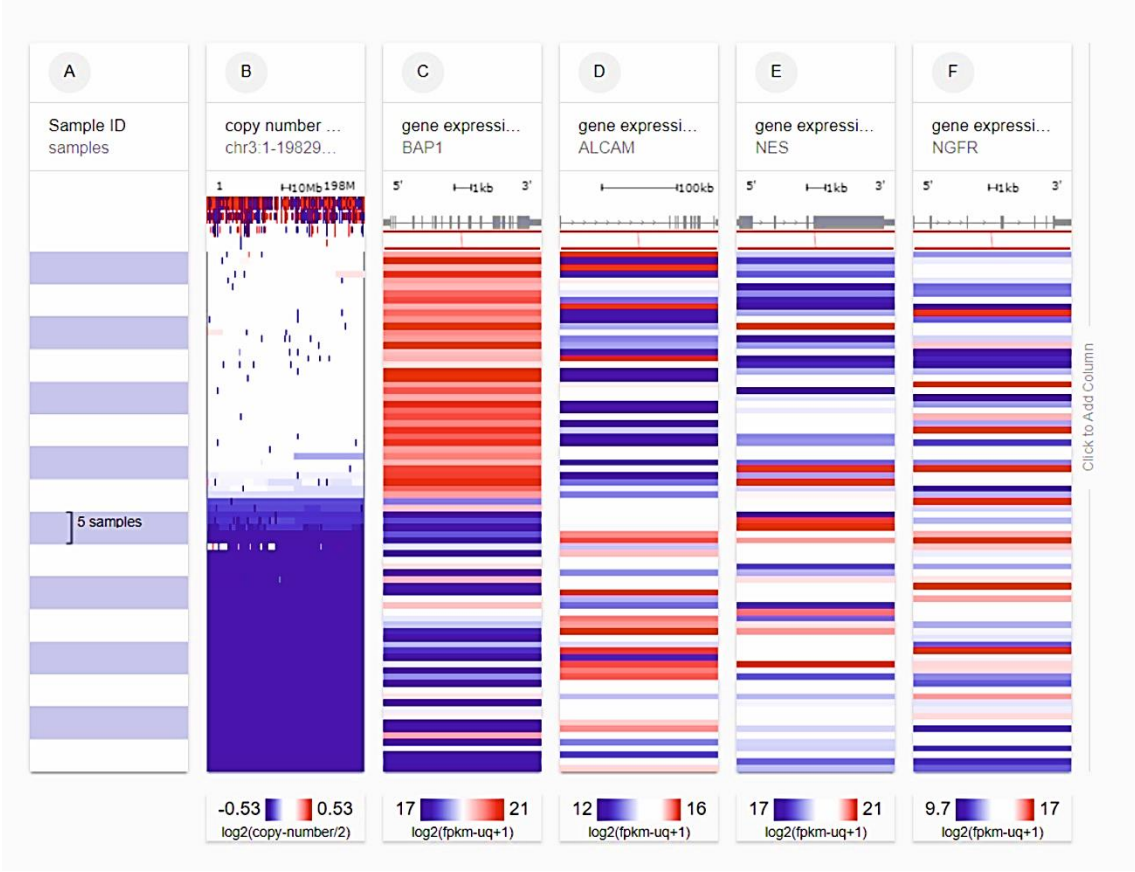

(II)

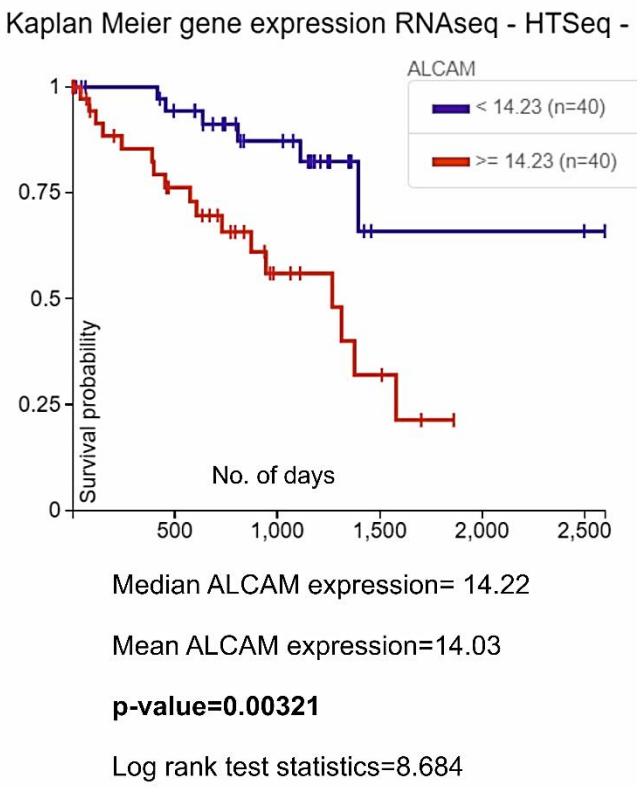

Figure 1.8. ***(I)****Heat map showing correlation between gene expression levels of* ***CD166/ALCAM***, ***Nestin*** *and* ***CD271/NGFR*** *to* ***BAP1*** *and* ***Chromosome 3 loss***. *The columns are* ***(A)*** *patient samples in rows,* ***(B)****chromosome 3 status,* ***(C)****BAP1* ***(D)****CD166/ALCAM* ***(E)****Nestin and* ***(F)*** *CD271/NGFR. Blue colour shows downregulation, red, upregulation and white shows median expression of a gene on a log scale. Upregulation of* ***CD166/ALCAM*** *expression was more abundant in* ***M3 UM*** *with* ***BAP1*** *downregulation while* ***Nestin*** *and* ***CD271*** *expression was variable across the 80 PUM samples.* ***(II)****Kaplan-Meier survival plot showing that* ***CD166/ALCAM*** *expression significantly correlates with overall survival, (p=0.0032).*

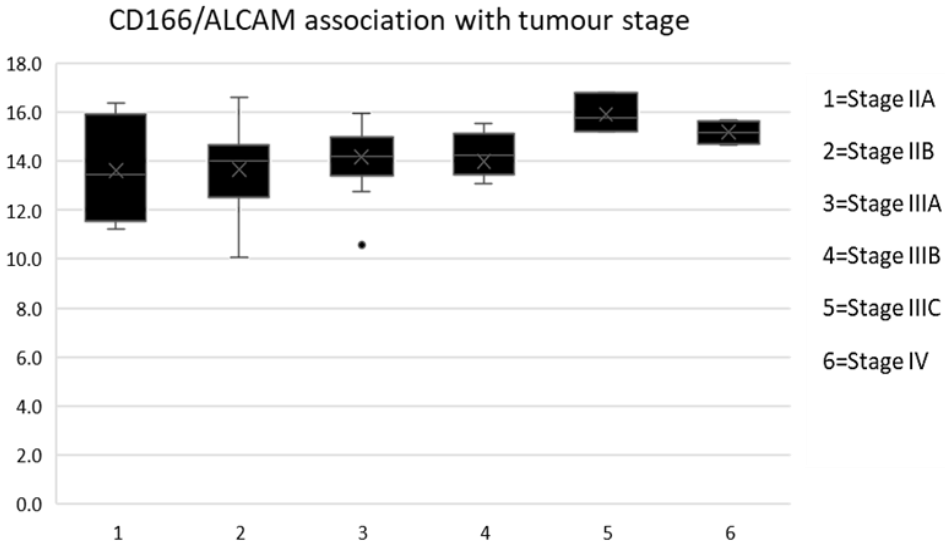

Figure 1.9. *CD166 gene expression levels plotted against AJCC TNM stages for UM patients included in the TCGA database. CD166 expression is may not be a covariate of the tumour stages.*

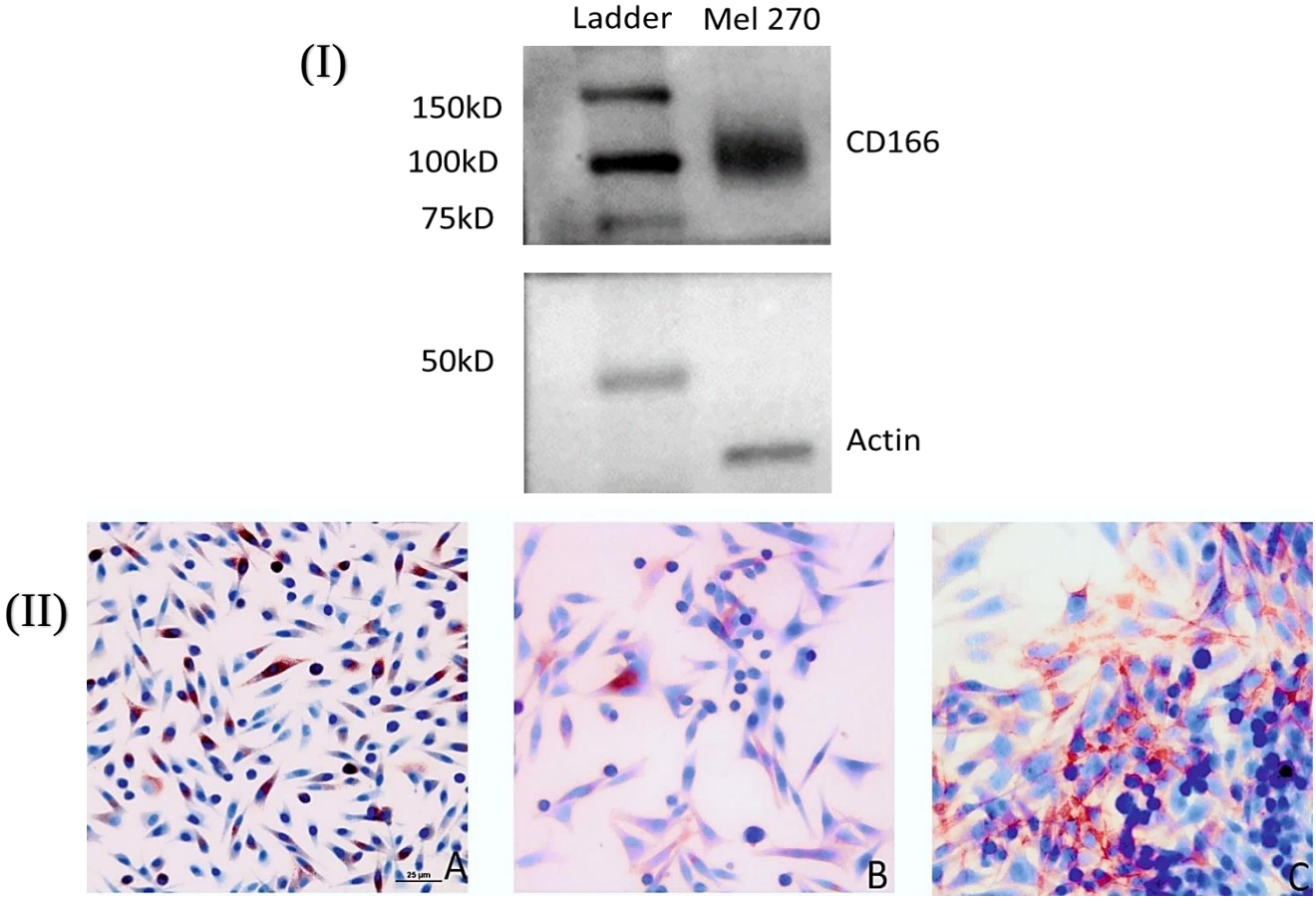

Figure 1.10. ***(I)*** *Western blot of CD166 protein in Mel270 cells. CD166 is detected at its predicted molecular weight (100-105kDa) while Actin is detected at 42kDa.* ***(II)*** *IHC expression of CD166 in the UM cell lines (A) 92.1, (B) Mel 270 and (C) OMM1 at 20x magnification.*

4.7. CD166^{high} Mel270 cells have a higher tumour transendothelial migration potential than CD166^{low} Mel270 cells

After obtaining distinct populations of CD166^{high} and CD166^{low} Mel270 cells by FACS **(Fig. 1.11 A),** the cells were plated on a layer of HUVEC cells cultured on transwell inserts with a 0.8µm pore size.

The HUVECs had been in culture for three days and had formed a confluent monolayer with tight junctions between the cells. Serum was used as a chemoattractant in the media, with a gradient of 1% serum on top and 10% serum at the bottom. The cells with CD166^{high} expression (mean 25,531, median 25,474, range:17,514-3363) migrated across the HUVEC layer more than those with CD166^{low} expression (mean 20,100, median 20,031, range: 17,617-22,474). A Mann-Whitney test showed that the differences were statistically significant, **p=0.015** (**Fig. 1.11 B**).

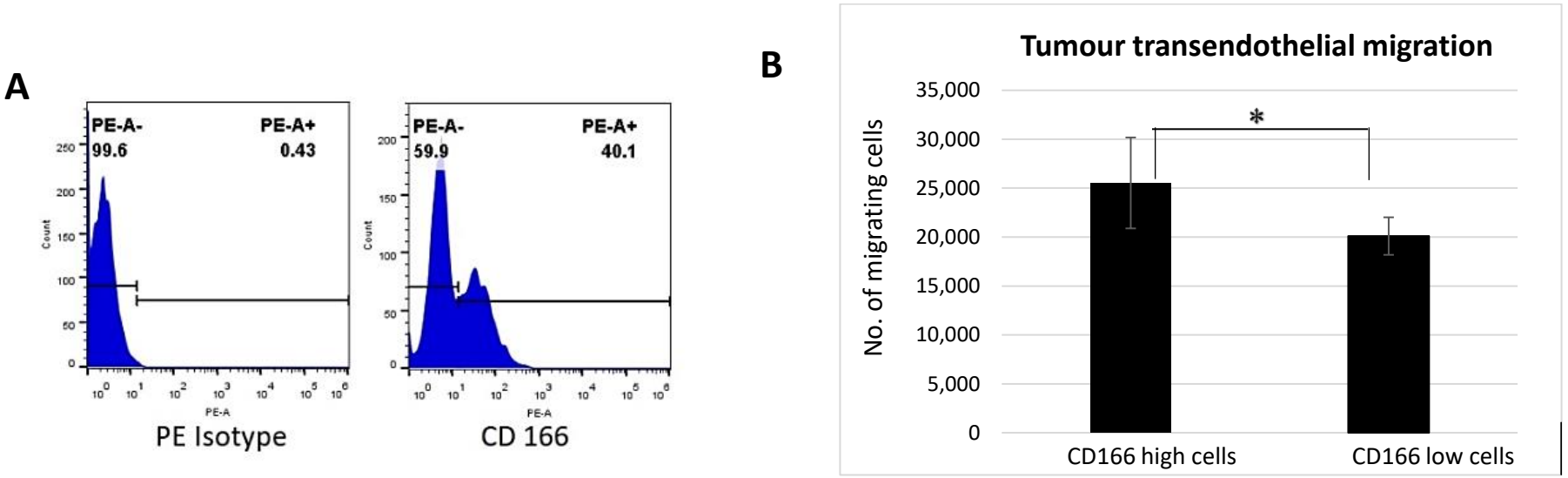

Figure 1.11. (A) *Flow cytometry profile of Mel 270 cell line. The cells positive for CD166 (40.1%) are shown.* ***(B)*** *Bar graph representing the number of Mel270 tumour cells migrating across the HUVEC and the insert layer. The experiment had six technical replicates and Mean±SD is shown. A Mann-Whitney test shows that extravasation was significantly (*) higher in CD166^{high} compared to CD166^{low} cells, p=0.015.*

4.8. CD166 is expressed in the cornea, ciliary body and optic nerve

IHC staining undertaken in eyes enucleated due to the presence of UM, revealed several normal ocular structures that expressed CD166. These served as an internal positive control when examining the tumour cells. They include the corneal epithelium, ciliary processes and ciliary muscle, trabecular meshwork and the meningeal layer of the optic nerve (**Fig. 1.12).**

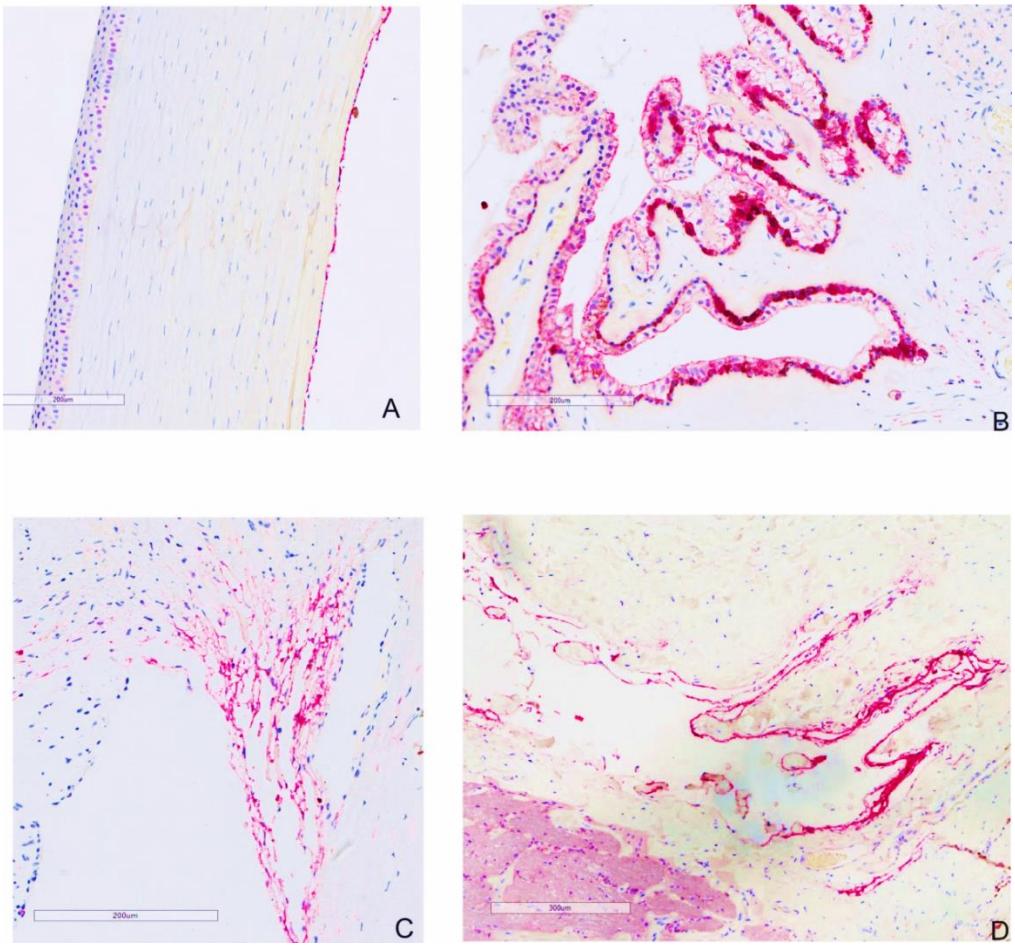

***Figure 1.12**. Representation of the CD166^{+} structures in the eye. (**A**) cornea epithelium; (**B**) the ciliary processes; (**C**) trabecular meshwork; and (**D**) the meningeal layer of the optic nerve.*

4.9. IHC analysis shows that CD166 is expressed in the PUM tissue.

IHC staining was performed in FFPE sections obtained from enucleated eyes of PUM patients. These are the same tumour samples used for STC and subsequent analysis by flow cytometry. The antibody used for IHC (Abcam: ab109215) was different than that used for flow cytometry (Biolegend: 343904) and was optimised before use. The specificity of this

antibody was also examined by Western blot as shown above. Melan A-stained slides of these tissue sections were obtained from the pathology archives and used to identify the UM cells. The identified PUM cells were then examined for CD166 expression.

PUM cells stained for CD166 in both the cytoplasm and the membrane. This was clearly observed in only two of the nine samples examined (eight were from enucleations and one was from an endoresection). In one of the samples, the staining was weak and involved only the anterior one-third of the tumour (**Fig. 1.13 A, B)**. In this region, 70% of the UM cells stained positive for CD166 while tumour cells in the posterior two-thirds of the tumour were negative. It was difficult to determine cytoplasmic or membranous staining in the heavily pigmented or macrophage dense UM sections (4/9).

In addition to positive staining for CD166 in the tumour cells it was also detected in the cytoplasm of the tumour associated macrophages **(Fig. 1.13 C)**. Normal pancreas sections stained positively for CD166 in the islets of Langerhans (**Fig. 1.13 D**). The NCM expressed membranous and cytoplasmic CD166 (**Fig. 1.13 E**). Endothelial cells in some tumour sections also stained positive for CD166 (**Fig. 1.13 F).**

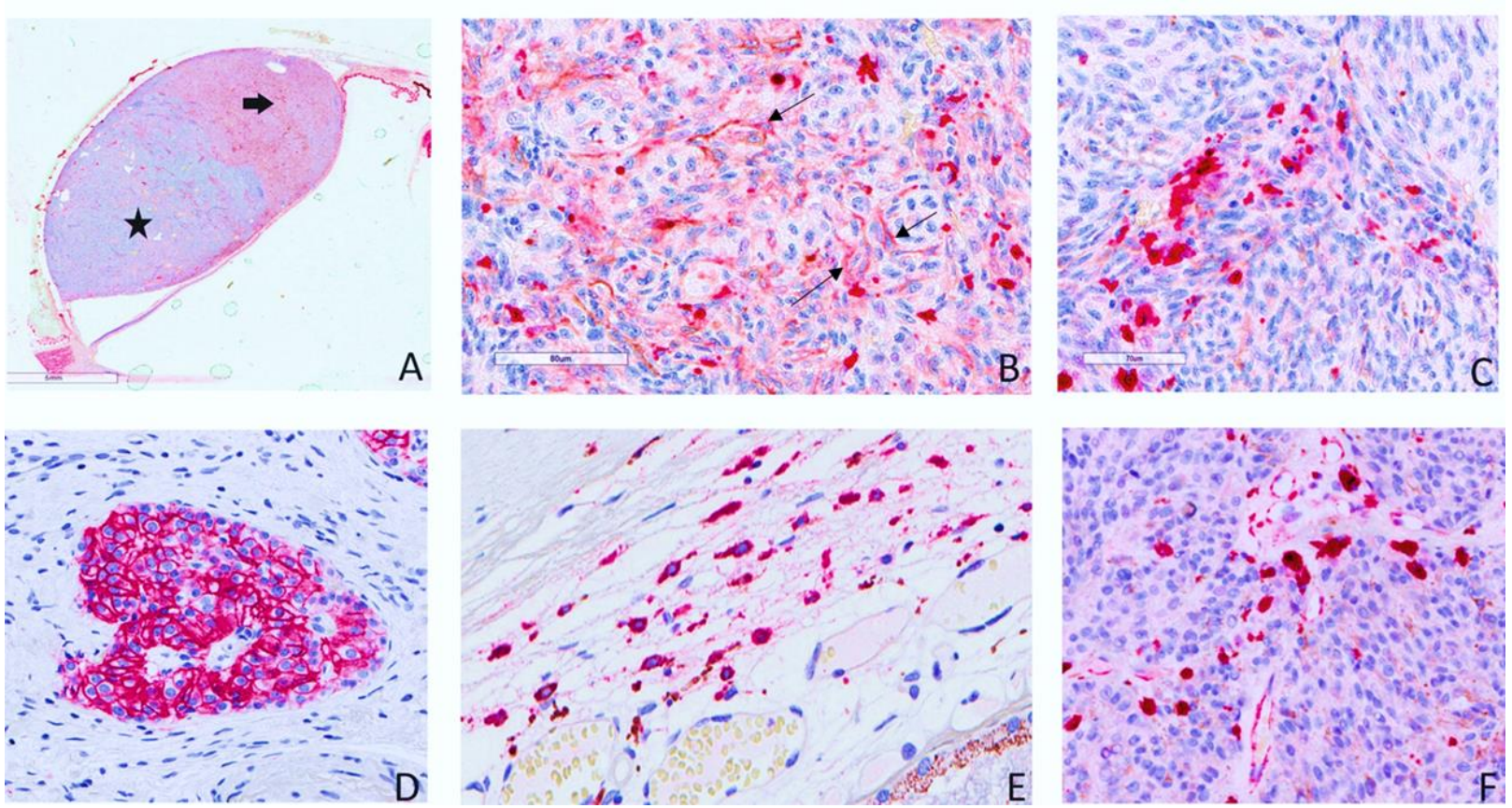

Figure 1.13. *(**A**) PUM tissue from an enucleated eye with positive staining for CD166 in the anterior one-third (bold black arrow) and negative staining in the posterior two-thirds (star) are shown. (**B**) Higher magnification of the anterior region showing membranous (thin black arrows) and cytoplasmic staining of PUM cells. (**C**) Posterior two-thirds (star) shows the negative staining of PUM cells and positive macrophage CD166 stain. (**D**) Positive control stain in the pancreas. (**E**) CD166 positive normal melanocytes. (**F**) Positively-stained endothelial cells and macrophages from the PUM tumour section.*

4.10. Neural crest markers are expressed in PUM

Evidence from skin melanoma shows that similar pathways and features are employed during malignant transformation and metastasis as those found in the embryonic NC cells. These include EMT, migration through different microenvironments and expression of NC regulatory factors/markers (90). Our hypothesis was that UM cells reactivate developmental pathways that control cell proliferation and migration. One of the aims of this study was to investigate if the developmental/neural crest markers are expressed in UM tissue. We focused on MITF, SOX10, PAX3, Notch 1 and Nestin, all which play a role in melanocyte development as shown below in (**Fig. 1.14).**

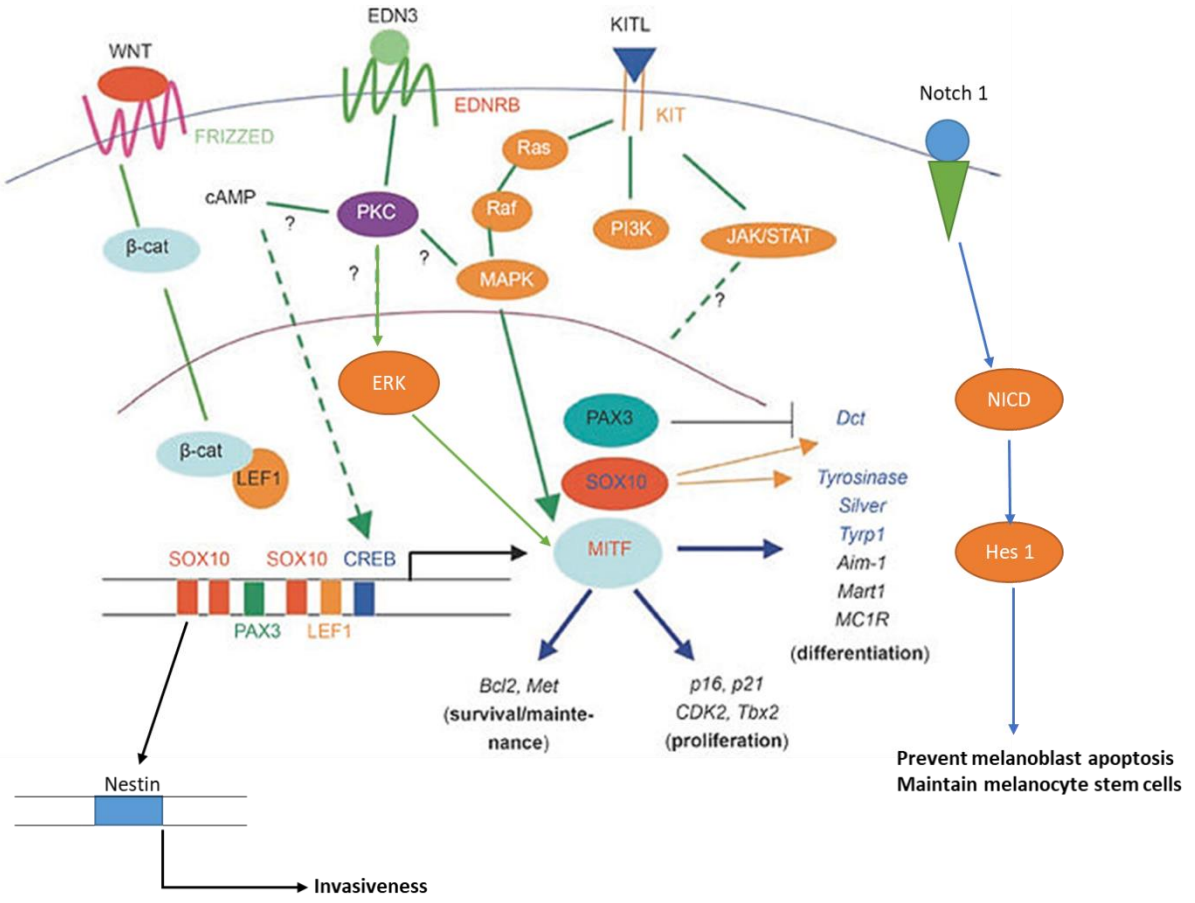

Figure 1.14*. Key regulatory signalling pathways involved in melanocyte development. Wnt, End3 and KIT activate MITF expression which then leads to melanocyte proliferation, survival and differentiation. Notch1 prevents apoptosis of melanoblasts and maintains melanocyte stem cells. SOX10 enhances Nestin gene expression resulting in increased migration and invasiveness of melanoma cells (Image adapted from Hou L et al. 2008(91)).*

IHC analysis showed that MITF, SOX10 and PAX3 are expressed in the nuclei of >80% of PUM cells in all six samples. The Notch1 antibody used detects activated Notch1 and is thus used to mark nuclear Notch 1 expression. Activated Notch1 was also expressed in the nuclei of >80% of PUM cells in all six samples (**Fig. 1.15**). There was no difference in the expression pattern of these markers when high-risk M3 tumours were compared to the low-risk D3 tumours. Poor prognostic features such as the presence of loops and epithelioid cells were seen in some of the M3 tumours, but this did not influence the expression of these markers.

C-KIT was expressed on the cell membrane of PUM in both the M3 and D3 tumours. It was expressed in >70% of cells in the M3 tumours and <50% of cells in the D3 tumours. Nestin was expressed only in the endothelium of the blood vessels of the D3 samples, with no expression in the tumour cells (**Fig. 1.15**). In the M3 UM, Nestin expression was evident in the membrane and cytoplasm of the tumour cells. Of the markers examined, C-Kit and Nestin showed variation in expression between the high and low metastatic risk tumours.

Overexpression of C-KIT in UM has been previously described (92) and a therapeutic agent (imatinib mesylate) acting against this tyrosine kinase inhibitor has been tested in a phase II multicentre clinical trial involving patients with unresectable MUM. The trial showed no effect of the drug and the clinical trial did not proceed to the next stage (93). Further investigations to the mechanism responsible for drug resistance in this trial showed that stem cell factor (SCF), a cytokine produced in the hepatic tumour microenvironment mediated imatinib resistance by competitively binding to the KIT receptor. This binding led to a conformational change of the receptor preventing stable binding of imatinib mesylate (93).Although C-KIT expression showed variation between M3 and D3 tumours in this study, it was not examined further. An investigation of Nestin, which had showed a distinct difference between M3 and D3 tumours was undertaken in a larger cohort of PUM samples, MUM and UM cell lines.

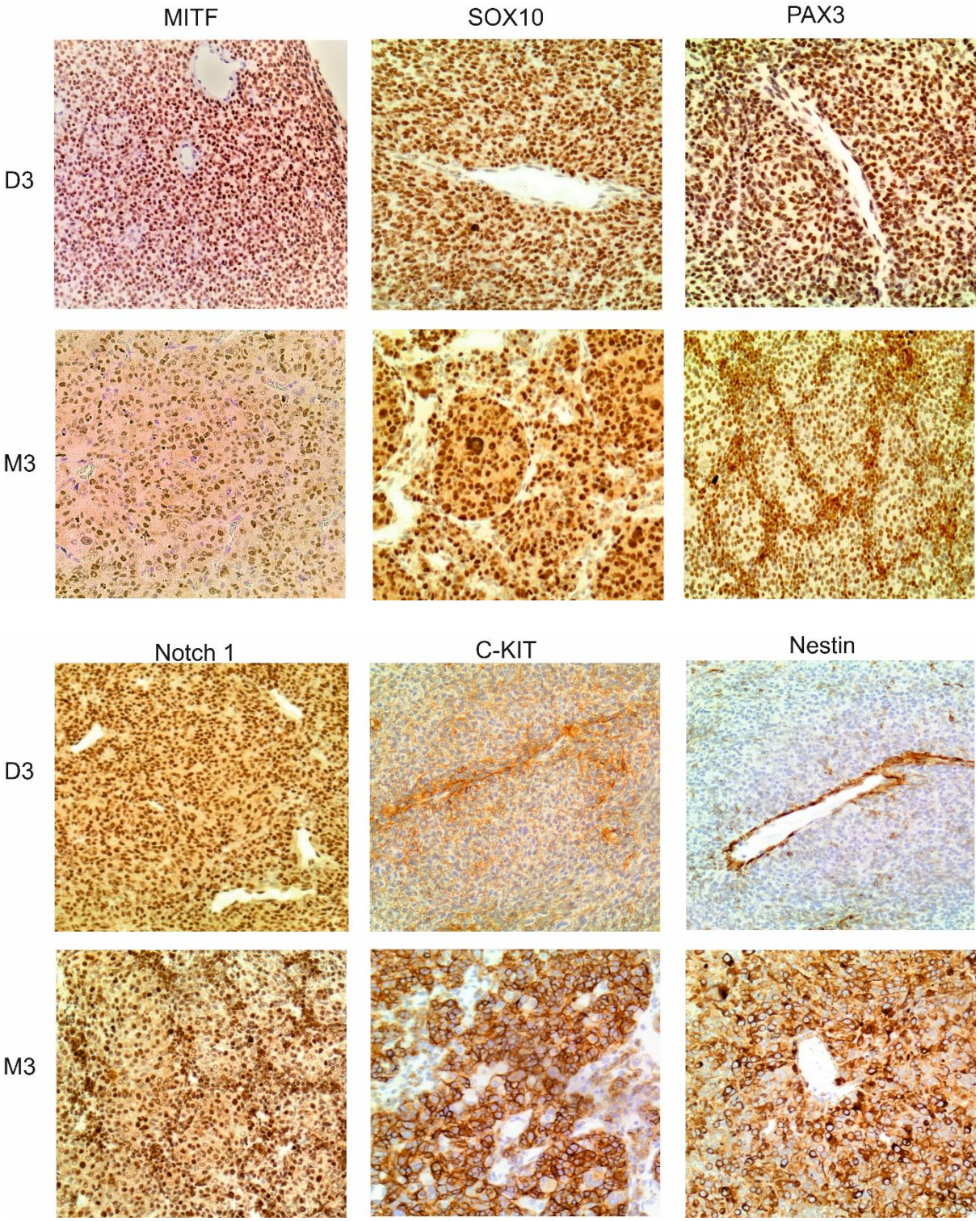

Figure 1.15. *Neural crest markers are expressed in PUM tissue. MITF, SOX10, PAX3 and Notch 1 are expressed in the nucleus of the PUM cells. C-Kit and Nestin are expressed in the membrane of PUM cells. D3 =Disomy 3 and M3= Monosomy 3. DAB chromogen (brown) was used to indicate positive staining and images were taken at 10x magnification.*

4.11. Nestin expression *in vitro*

A western blot was performed using two UM cell lines to determine the specificity of the Nestin antibody used. Nestin was expressed in the Mel270 and MM66 UM cell lines. It is visible at a higher molecular weight (~250kDa) (**Fig. 1.16**) than the predicted 177kDa, however this is consistent with data provided by the manufacturers and also as reported on www.proteinatlas.org/ENSG00000132688-NES/antibody, which reports a WB band of around 250kDa and interaction of the antibody only with its own antigen on protein array. A preliminary IHC staining of six UM cell lines was also undertaken. Nestin was expressed in the cytoplasm as well as the membrane of these cell lines (**Fig. 1.16).** Following this a large cohort of PUM samples (144) were stained for Nestin.

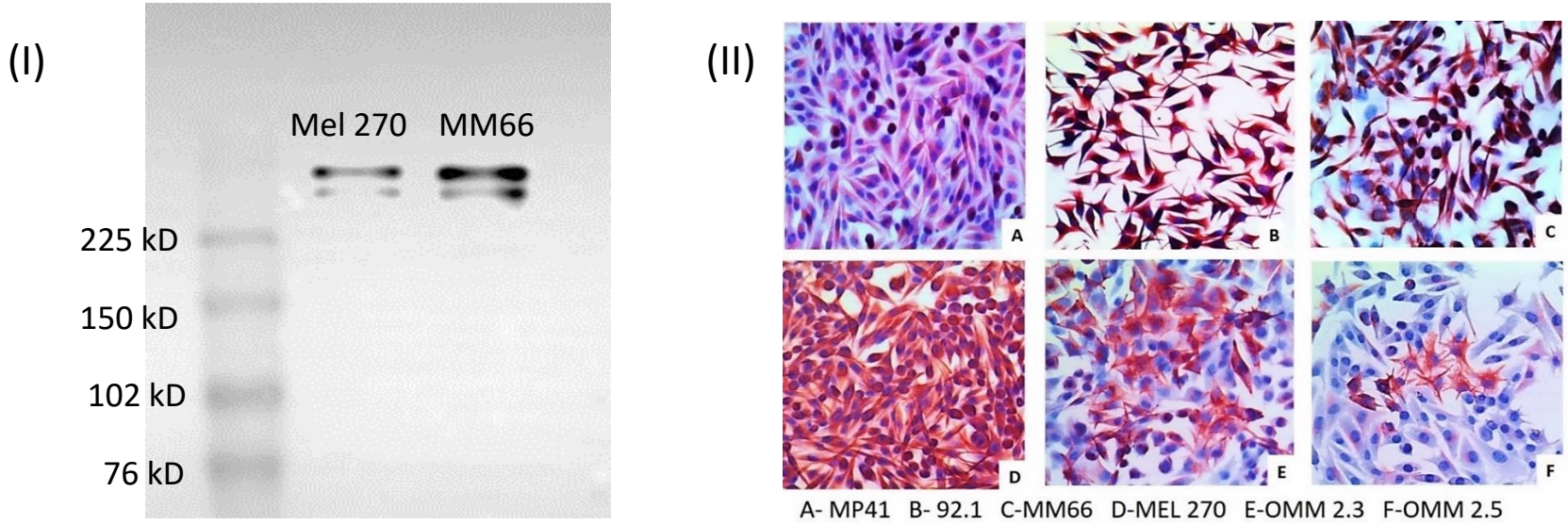

Figure 1.16. *(**I**) Western blot showing Nestin expression in Mel270 and MM66 UM cell lines. (**II**) Nestin protein expression as determined by immunocytochemistry in the cytoplasm and membrane of six UM cell lines. Positive staining is shown by AEC chromogen (red). Images were taken at 10x magnification.*

4.12. Nestin expression in PUM

144 PUM samples underwent IHC staining for Nestin. The results were scored on a 0-100% scale for positively stained tumour cells. Nestin was positive in several non-tumour areas of the globes and these were used as positive internal controls to validate the IHC stain alongside the normal control colon sections. These areas include the cells of the neuroretina, the inner and outer nuclear layer, the ganglion cells and optic nerve fibre layer (**Fig. 1.17A**). The blood vessels were also Nestin positive. The retinal pigment epithelium and the NCM did not express Nestin **(Fig. 1.17, B**).

Melan A-stained slides of the tissue sections obtained from the pathology archives were used to identify the UM cells across the tissue sections, and to determine the quality of immunostaining of the samples following formalin fixation. The identified UM cells were then examined for their Nestin expression. The UM cells expressed Nestin in their membrane and cytoplasm. The endothelium of the intratumoural blood vessels were also positive for Nestin in some tissue sections **(Fig. 1.17D).** To determine the highest levels of sensitivity and specificity for Nestin expression, a ROC analysis was performed. The data identified that a range of expression between 8.5% (0.857/0.584; sensitivity/specificity) and 12.5% (0.679/0.478; sensitivity/specificity) would give the highest sensitivity and specificity respectively at 95% confidence interval (CI). A 10% threshold was therefore used as the cut-off point. Previous studies examining Nestin had also used this threshold (94). UM samples with <10% Nestin expression (**Fig. 1.17C)** were thus considered negative for this marker.

Fifty-two of 141 (36%) of the examined PUM were scored as negative for Nestin expression. Sixty-three PUM (44%) showed varying intensity of Nestin expression ranging from 10-50% positivity in the tumour cells (**Fig. 1.17 E, F).** Nestin was expressed in 50– 100% of UM cells in the remaining 26 PUM samples (18%). In these samples, Nestin was expressed both in the cytoplasm and membrane of cells **(Fig. 1.17 G, H).** Positive staining in the endothelium of the intratumoural blood vessels was observed in a total of 36 PUM (25%).

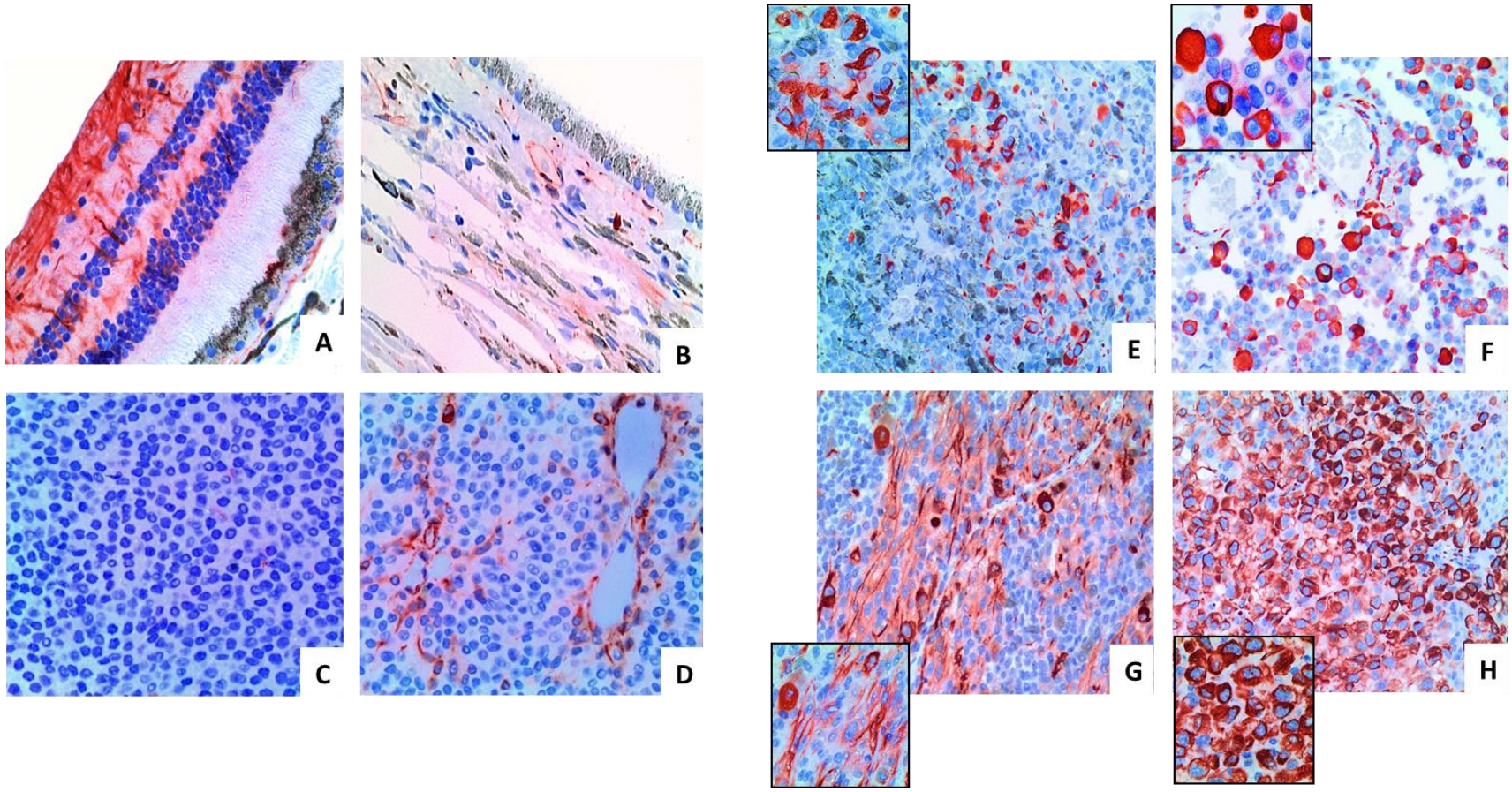

Figure. 1.17. ***(A)*** *Nestin expression in the neuroretina, inner, outer nuclear layer and the optic nerve layer.* ***(B)*** *The choroidal melanocytes and retinal pigment epithelium are negative for Nestin.* ***(C)*** *PUM tissue section with <10% of tumour cells expressing Nestin.* ***(D)*** *The intratumoural capillary endothelium tissue expressed Nestin.* ***(E, F)*** *PUM tissue sections expressing Nestin in 10–50% of the cells.* ***(G, H)*** *Nestin expression in >50% of cells (All images are at 10x magnification). Insets show staining at (40x magnification).*

4.13. Survival analysis

When correlated with known poor prognostic factors in PUM (58-60), Nestin positivity (≥10%) was significantly associated several predictors of metastasis. These include epithelioid morphology (Pearson's Chi-square $p<0.0001$), high mitotic count (Mann–Whitney $p<0.0001$), closed connective tissue loops (Pearson's Chi-square $p=0.001$) monosomy 3 (Pearson's Chi square $p=0.007$) and chromosome 8q gain (Fisher's exact test $p<0.0001$). Increasing Nestin expression was significantly correlated with the absence of nBAP1 protein expression ($p=0.015$, Mann–Whitney) (**Fig. 1.18A**). Nestin expression in the capillary endothelium showed no significant correlation with any prognostic factor. Patients with PUM classified as negative for Nestin expression (<10%) had a better prognosis than those patients with positive Nestin expression in the tumour cells as shown by the Kaplan–Meier analysis (**Fig. 1.18B**; Log-rank $p = 0.002$).

4.14. Nestin expression in MUM

Melan A-stained slides of MUM were obtained from the Pathology archives and assessed, similarly to the PUM described above. They were used as a reference to show the antigenicity of the tissue and to identify the tumour cells. The hepatocytes and hepatic stellate cells did not express Nestin while the MUM cells and associated blood vessels were positive for Nestin. nBAP1 data were available for 19 of the 26 MUM; 17 MUM were negative for nBAP1 expression and two were positive for nBAP1.

50-100% of Nestin positive tumour cells was were seen in ten of the 26 MUM (38%) (**Fig. 1.19 A**). Nine of the 26 samples (34%) had 10-50% of Nestin expressing cells. In 17 (65%) of the samples, Nestin was expressed in the UM cells located within closed connective tissue loops (**Fig. 1.19 B**). Six (23%) of the 26 MUM had <10% Nestin-expressing tumour cells (**Fig. 1.19 C**), and in one other, Nestin expression was completely negative. Nestin expression in the intratumoral capillary endothelium was visible in nine MUM samples which also showed a high proportion (50-90%) of Nestin-positive melanoma cells in the tissue (**Fig. 1.19 D**).

A

Variable	*<10% Nestin*	*>10% Nestin*	*p-value*
Age			
Median	63.5(28-86)	62(20-87)	0.463*
Gender			
Male	30	52	0.932*
Female	22	37	
LBD(mm)			
Median	15.1(3.3-23.6)	15.2(5.9-22.5)	0.109¥
UH(mm)			
Median	7.8(1.4-16.7)	8.6(1.7-16.6)	0.287¥
CBI			
Yes	14	37	0.081*
No	38	52	
EOE			
Yes	3	13	0.110¥
No	49	76	
Epithelioid cells			
Yes	19	68	P-*
No	33	21	
Closed Loops			
Yes	22	64	**0.001***
No	30	25	
Necrosis			
Yes	6	19	0.141*
No	46	70	

Variable	<10% Nestin	>10% Nestin	p-value
Mitotic Count(40/hpf)			
Median	2(0-38)	5(1-23)	P-†
Chr 3 status			
Loss	26	63	**0.007***
Normal	23	20	
Unclassifiable	3	6	
Chr 8q status			
Loss	6	5	P-¥
Normal	25	17	
Gain	17	64	
Nuclear BAP1			
Yes	28	39	0.250*
No	24	50	

¥ Student T test
† Mann-Whitney test
*Pearson Chi- square
¥ Fishers Exact Test
Boldface values indicate statistical significance ($P \leq 0.05$).

B

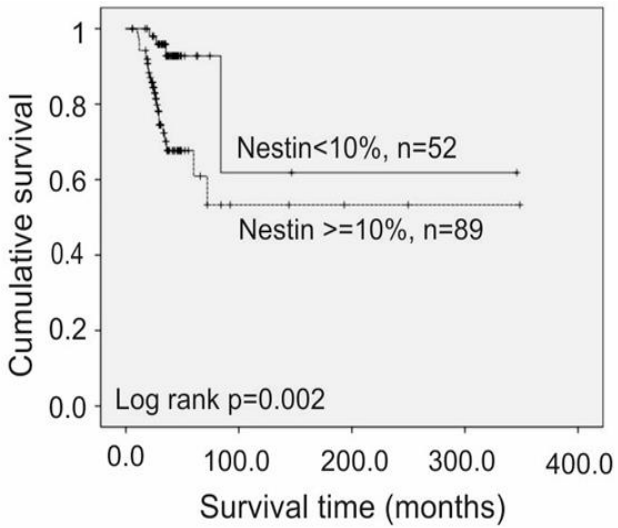

Nestin Positivity	Total No. of Sample	No. of Events	Censored		Mean survival time(Months)	Std. Error	95% Confidence Interval	
			No.	Percent			Lower Bound	Upper Bound
<10%	52	4	48	92.3%	242.007	66.797	111.085	372.929
= 10%	89	24	65	73.0%	203.074	30.074	144.130	262.019
Overall	141	28	113	80.1%	226.494	28.066	171.484	281.503

Figure 1.18. (A)*Correlation of Nestin with clinical and prognostic factors. LBD= Largest basal diameter, UH=Ultrasound, CBI=Ciliary body involvement, EOE= Extraocular spread.* ***(B)****Kaplan–Meier survival curve and table for all PUM stratified according to Nestin expression. Nestin expression ≥10% was associated with poor outcome (****Log rank p=0.002****). No. of events indicates the number of deaths from metastatic UM.*

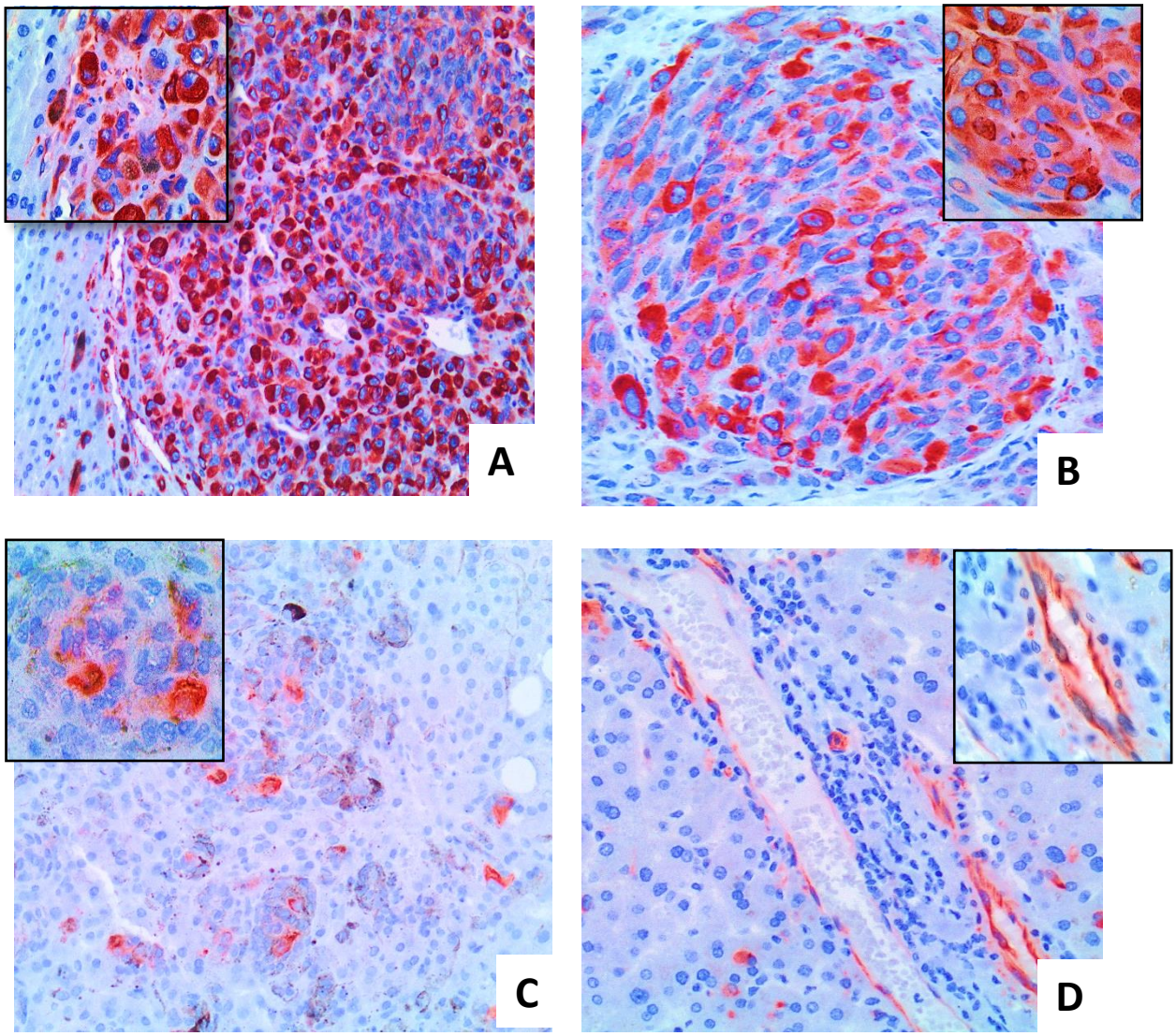

***Figure 1.19**. Representative images of Nestin expression in MUM (10x magnification). Insets show Nestin expression at 40x magnification. (**A**) and (**B**) show a high proportion of Nestin-expressing UM cells both inside closed connective tissue loops and outside. (**C**) shows only a few Nestin-positive cells, while (**D**) shows Nestin expression in the capillary endothelium of the MUM.*

4.15. Nestin expression in matched PUM-MUM

Scattered UM cells that were located away from the bulk of the tumour in the MUM sections also stained positive for Nestin. Eleven of the MUM samples had matched PUM sections available. When examined, Nestin was expressed in the cytoplasm of the UM cells in all the PUM tissue sections **(Fig. 1.20B**). In one (9%) PUM, there were <10% of Nestin positive cells in the tumour section. Eight (72%) of the eleven PUM had 10-50% of Nestin expressing cells while in the remaining two samples (18%), Nestin was expressed in 50-90% of the PUM cells. In five of these PUM samples, staining was also seen in the intratumoural capillary endothelium. Nine of these matched PUM were negative for nBAP1 expression, one was positive and for one, data were not available.

A varied expression of Nestin was seen in the MUM: four MUM (36%) expressed Nestin in >50% of the tumour cells (**Fig. 1.20D**), three (27%) expressed Nestin in 10–50% of UM cells. In two (18%) other samples, only scattered large ovoid MUM cells stained positive for Nestin (**Fig. 1.20H**). Only the intratumoural capillary endothelium stained positive for Nestin in the remaining two samples (18%). Seven of these MUM were negative for nBAP1 expression, two were positive while the BAP1 expression data were unavailable for the remaining two samples.

Interestingly, three of the four MUM samples with >50% of cytoplasmic Nestin-expressing cells had shorter metastasis free and overall survival than the MUM in which Nestin expression was <50%. One of the patients died 2 weeks after the diagnosis of metastatic melanoma while the two others died within one month of diagnosis. The fourth patient is still alive with features of good prognosis such as nuclear BAP1 expression in the PUM and a normal (disomy) chromosome 3 status. The MUM cells in the liver resection are also nBAP1 positive for this patient. The three-remaining matched M3 PUM and MUM were negative for nBAP1 expression.

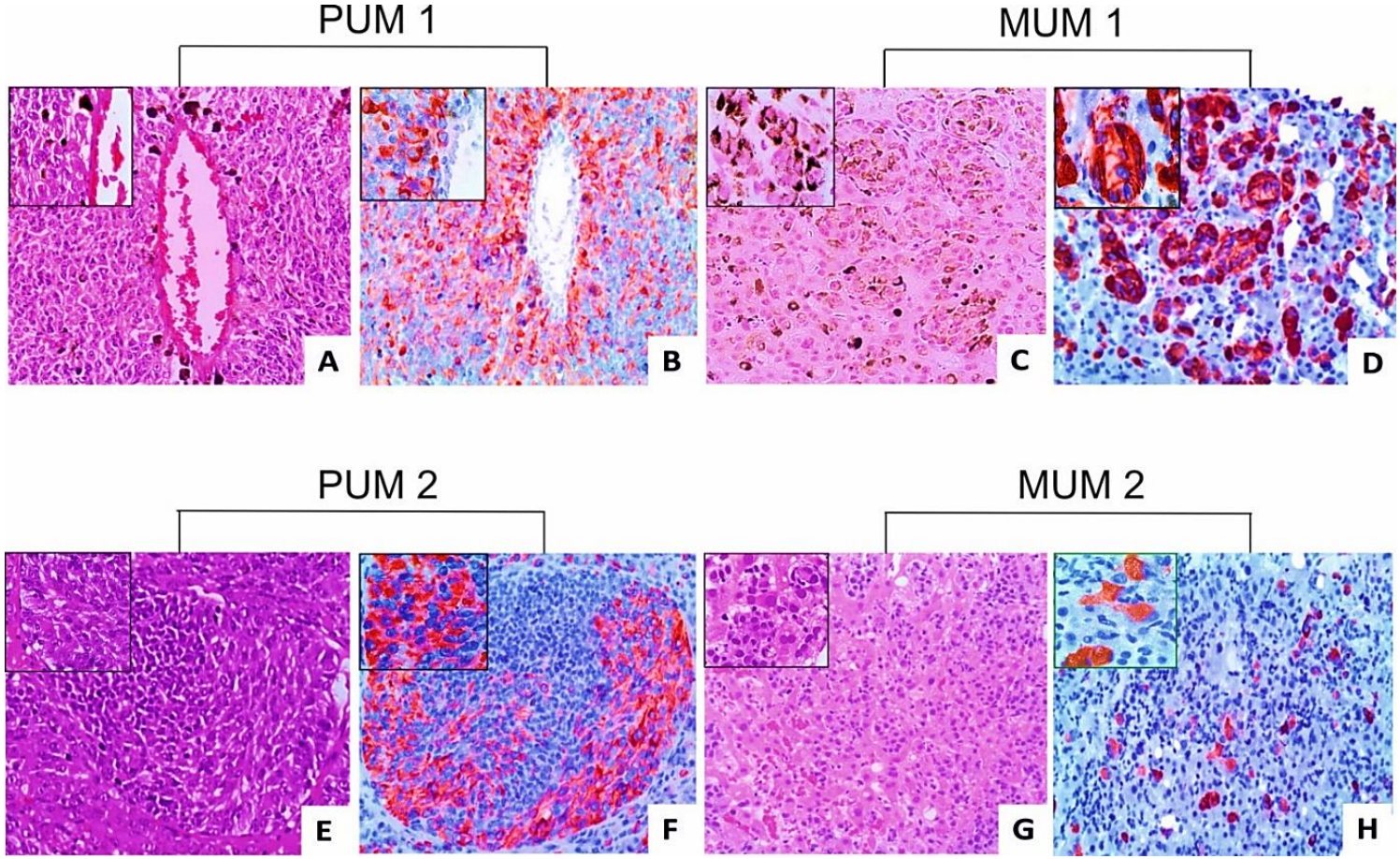

Figure 1.20. *Nestin expression in two representative matched PUM-MUM.* ***A, C, E*** *and* ***G*** *are H&E-stained images.* ***B, D, F*** *and* ***H*** *show Nestin expression. A high proportion (>50%) of Nestin-expressing tumour cells are seen in both (**B**) PUM1 and (**D**) MUM1 from the same patient. Nestin expression was noted in tumour cells of (**F**) PUM2 contained within large closed connective tissue loops. (**H**) MUM2 showed Nestin expression in large ovoid tumour cells. PUM2 and MUM2 are from the same patient.*

5.Discussion

This study has shown the expression of CSC markers in UM. Flow cytometry results have demonstrated increased expression of the CSC markers, Nestin, CD271 and CD166 in high metastatic risk PUM compared to low metastatic risk PUM and NCM. The ability of a subpopulation of UM cell lines to escape anoikis by upregulating stemness markers such as CD166, CD271 and Nestin provides further evidence for the existence of CSCs in UM. This study has also shown that protein markers associated with NC developmental pathways leading to melanocyte specification are expressed in UM, suggesting that these primitive pathways may be reactivated in this tumour. These markers, including MITF, SOX10, PAX3, Notch 1, C-KIT and Nestin, have been shown to play a role in the tumourigenesis and metastasis of several cancers, particularly skin melanoma. They may function in a similar manner in UM.

Studies in skin melanoma have shown a higher overall expression of CD166 in primary tumours than benign lesions by IHC (95, 96). Consistent with these studies, flow cytometry analysis showed that PUM expressed more CD166 compared to NCM. Nestin expression was also higher in the PUM compared to the NCM, consistent with previous reports in literature (82). The findings of Lai et al. who examined expression of CD146/MCAM/MUC18 in the uvea support the CD146 results in this study (97). They reported that CD146 is expressed in the NCM, FFPE tumour sections and UM cell lines. This membrane marker has since been included in the FDA-approved Cell Search system for isolation of circulating melanoma cells in the blood (98, 99). However, the high levels of expression of this marker in both UM and NCM suggest that it lacks specificity as a CSC marker.

Anoikis is an apoptotic cell death process induced in cells after their detachment from the extracellular matrix (ECM) (100). It is a physiological process that prevents attachment and seeding of displaced cells at inappropriate sites. Resistance to anoikis is a hallmark of tumorigenesis and metastasis, as it enables cancer cells to survive and spread in the blood or lymphatic system (100). The different causes of anoikis resistance in cancer cells, include genetic instability, intra-tumoral hypoxia, epithelial-mesenchymal transition and overexpression of stemness markers (101). Overexpression of stemness markers activates processes including cell proliferation, survival, motility, migration, apoptosis and anoikis resistance (100). CSCs in several cancers including breast have been shown to be resistant to

anoikis, form spheres in non-adherent culture and have enhanced tumour growth capacity (102).

In this study, UM cell lines surviving anoikis showed an increased expression of several markers previously associated with neural crest development and stem cells: CD271, Nestin and CD166. The CSC population in skin melanoma has been shown to express CD271 (103). Samples having >5% of CD271/SOX10 positive cells correlated with poor tumour specific survival. $CD271^{+}$ cells were able to form tumours in xenograft models that resembled the parent tumour. The range of CD271 expression was 4.1-5.9% in these tumour cells from passage one to passage five xenografts (103). In UM, CD271 was also expressed in the cells that formed vasculogenic mimicry patterns, a poor prognostic feature likely to cause metastasis (20). In this study, CD271 was upregulated (median 8.9%) in the cells surviving anoikis compared to cells in adherent culture (median 1.0%). Its expression was also higher in M3 tumours (median 6.8%) compared to D3 tumours (median 4.5%) suggesting its role in selecting for the CSC population.

Nestin was identified as a marker of skin melanoma stem cells along with CD133 and CD166. It was expressed at moderate to strong intensity in >15% of cells of the primary and metastatic melanomas but not nevi (95). Nestin protein and mRNA expression were also described in UM cell lines and primary tissue in the study investigating putative CSCs in UM. The $CD133^{+}$/$Nestin^{+}$ cells ranged from 3.1-17.6% in Mel270, OMM2.3 and OMM2.5 UM cell lines by FACS analysis (104). Although the $CD133^{+}$/$Nestin^{+}$ double positive cells were not examined in this study, the presence of Nestin in the UM cell lines supports the findings of the study by Thill et al (104). These results suggest that PUM cells surviving anoikis may be enriched by the CSC population, as evidenced by their increased expression of stemness markers.

In the PUM tissue sections stained by IHC, CD166/ALCAM expression was abundant in the cytoplasm of the tumour associated macrophages. These results support those of Levesque et. al who showed that CD166/ALCAM is expressed in the macrophages of arthritis patients in response to cytokine release (105). Variable CD166 staining was also observed in macrophages in the study by van Kempen et al. examining ALCAM expression in skin melanoma (89). Tumour endothelial cells also expressed CD166/ALCAM, which has been reported to be involved in early embryonic haematopoiesis and vasculogenesis (106). In this study, expression of CD166/ALCAM in the PUM cells analysed by IHC was not as abundant

as demonstrated by flow cytometry. The presence of CD166 positive macrophages and endothelial cells may account for this. However, its location was similar to that in skin melanoma, being positive both in the membrane and the cytoplasm of the tumour cells (89).

CD166/ALCAM was expressed in several normal structures of the eye including the normal choroidal melanocytes. This had only been previously reported in the choroid of mice although its role is yet to be established (107). The ciliary muscle and ciliary processes also strongly expressed ALCAM in their membrane. Additionally, the trabecular meshwork also had ALCAM positivity. Implications of the glaucoma disease process and possible drugs may be drawn from these results. Expression of ALCAM in the corneal endothelium has previously been reported, both *in vivo* and *in vitro* (108, 109). Similarly, ALCAM is important in neurogenesis and in supporting neurite extension (110). It is expressed in spinal cord motor neurons and those of the peripheral nervous system (111). Its expression in the body and meninges of the optic nerve was therefore anticipated. Further investigations are necessary to ascertain if these data may be of clinical relevance. Our findings also present new insights into the expression of CD166 in the other structures of the eye, which have not been reported previously.

In this study a detailed examination of Nestin expression in PUM and MUM was also performed. The results show that Nestin expression is associated with a reduced survival time in UM. Nestin expression also significantly correlates with known poor prognostic factors in PUM, such as epithelioid cell morphology, high mitotic count, the presence of closed connective loops, monosomy 3 and polysomy 8q.

Gene expression profiling has shown that these poor prognostic parameters are also associated with so-called high metastatic risk ‘class 2’ UM (112). These class 2 PUM express genes similar to those seen primitive neuroectodermal and neural crest cells. The authors suggest that class 2 PUM have cells with primitive stem-like cell phenotype (113). Nestin is expressed in the migrating and proliferating neuroectodermal cells during embryogenesis. In adult tissues, it may identify primitive multipotent cells with regenerative capacity that can be re-activated during injury (114).

The absence of Nestin positivity in NCM as compared to its presence in UM cells may suggest reversion to a more primitive phenotype during tumourigenesis. This theory may be supported by evidence from recent studies in several tumours, including cutaneous

melanoma, squamous cell carcinoma, basal cell carcinoma, osteosarcomas and gliomas (115-117) that have associated increased Nestin expression with an immature and invasive cell phenotype. Data from this thesis also supports these findings. Nestin expression was higher in the PUM compared to NCM as well as in M3 tumours (higher metastatic risk) compared to D3. The Nestin expressing UM cells may represent a subpopulation with stem cell-like characteristics.

In support of this, data generated by The Cancer Genome Atlas (TCGA)-UM study (53) and from the analysis of gene expression data previously generated by Laurent et al.(118), showed that Nestin mRNA expression was identified in a panel of genes associated with reduced time to metastasis after diagnosis of the PUM. However, this association was not found to be significant when examining the hazard ratio and 95% CI (118). This may be due to the relatively small cohort examined by the TCGA (n = 80), as compared to the 141 PUM examined in the current study.

The presence of putative CSC with self-renewal capacity that were resistant to chemotherapy was previously reported in UM cell lines (119). Nestin expression has been shown in the tissue of melanoma patients as well as in their circulating tumour cells (CTC). An analysis of the blood obtained from both cutaneous and UM patients revealed Nestin-expressing cells, which were absent in healthy volunteers (120). 17 skin melanoma patients with stage IV disease had Nestin mRNA expression in their blood samples compared to 4 stage III/II patients. Nestin mRNA expression was also significantly ($p=0.041$) higher in the blood samples of patients with high versus low tumour burden (121). This strongly proposes the possible use of Nestin as a biomarker for early detection of metastatic disease in high-risk UM patients. Its sensitivity may be more than that of previously proposed serum biomarkers, such as osteopontin, S100B and melanoma inhibitory activity (MIA). Nestin may be added to the panel of sensitive serum biomarkers of MUM along with the proposed cytokeratin 18 (122) and GDF-15 (123).

The molecular function of Nestin has also been investigated in several cancers. Suppression of Nestin expression by shRNA in cutaneous melanoma cell lines has been shown to lead to reduced cell growth, migration and invasion into Matrigel (124). These cells also have less spheroid formation ability than the control. When these cells were injected into mice, they formed smaller tumours, which did not metastasize to the liver (124). In gliomas, similar results were observed following Nestin knockdown (125). In pancreatic ductal carcinoma,

Nestin downregulation inhibited liver metastasis *in vivo* (126). In UM, further functional studies are necessary to help us to delineate the role of Nestin. In this regard, Nestin IHC has been undertaken in a panel of six UM cell lines to determine baseline expression of this protein. Several UM cell lines with high levels of Nestin expression (e.g. 92.1, Mel270 and MP41) have been identified. These may then be used to create isogenic cell lines for *in vitro* functional assays. These assays have been included in our future plans.

In conclusion, the present study shows that UM contains a population of cells with characteristics of CSCs *in vitro*. In particular, $CD166^{high}$ UM cells may represent a subpopulation with enhanced migratory capacity. Our future plans include using *in vivo* models to investigate if these findings can be recapitulated in living organisms. Additionally, this study has suggested that developmental pathways may be activated in UM cells, evidenced by the expression of NC and melanocytic lineage markers in PUM samples. PUM samples with >10% of Nestin-expressing cells correlate with poor survival. Nestin is also expressed in MUM, which together with previous studies showing Nestin expression in CTC, suggests that Nestin may be used as a biomarker in high-risk UM patients for early detection of disseminated disease. It is possible therefore that UM CSCs may be identified using several markers including CD166 and Nestin.

6. Acknowledgements

Firstly, I would like to thank my PhD supervisors **Prof. Goran Petrovski, Prof. Sarah Coupland** and **Dr. Helen Kalirai** for providing me with the opportunity to work in their labs, for teaching me many techniques, allowing me to present at numerous conferences and charting my course as a researcher. They have provided me with constant support and encouragement. I am forever grateful for knowing and working with them.

I would also like to thank **Prof. Andrea Facskó** for providing the institutional background that enabled me to commence my studies during my first year at the University of Szeged. I am sincerely grateful to **Prof. Andrea Varró** for organising the Dual Internationalisation program that facilitated my second and third year of the PhD at the University of Liverpool. It has been an honour to be part of the knowledge and skills exchange that has taken place due to the collaboration of the two universities.

I am grateful to my colleagues at the University of Szeged, without whom my journey as a researcher would not have started. I am grateful to **Dr. Richárd Nagymihály, Dr. Réka Albert, Dr. Natasha Josifovska, Dr. Dóra Szabó, Dr. Zoltán Veréb, Dóra Eszes and Dr. Renáta Gáspár** for their help and guidance. I offer my deepest gratitude to my colleagues at the University of Liverpool and all the present and past members of LOORG, namely, Dr. Karen Aughton, Dr. Sophie Thornton, Dr. Jodi Alexander, Dr. Alda Rola, Dr. Carlos Figueiredo, Dr. Jakub Khzouz, Prof. Azzam Taktak, Dr. Sam Prendegast, Dr. Jenna Kenyani, Dr. Ibrar Ahmed, Dilem Shakir, Debbie, Joanne, Dawn and Simon. Your constant support these two and a half years have propelled me forward and been enabled me to run this race.

Lastly, I would like to give my appreciation to my parents, siblings and extended family for the support, encouragement and sacrifices that they have made to set me on this path and walk along with me to this point. Without you I would not be here. Thank you.

7. References

1. R. EJ. Eye pathology: an atlas and text. 2nd ed. Philadelphia, PA Lippincott Williams & Wilkins,; 2011.
2. Singh AD, Topham A. Incidence of uveal melanoma in the United States: 1973-1997. Ophthalmology. 2003;110(5):956-61.
3. Yonekawa Y, Kim IK. Epidemiology and management of uveal melanoma. Hematol Oncol Clin North Am. 2012;26(6):1169-84.
4. Hu DN, Yu GP, McCormick SA, Schneider S, Finger PT. Population-based incidence of uveal melanoma in various races and ethnic groups. Am J Ophthalmol. 2005;140(4):612-7.
5. Al-Jamal RT, Kivela T. Uveal melanoma among Finnish children and young adults. J AAPOS. 2014;18(1):61-6.
6. Nickla DL, Wallman J. The multifunctional choroid. Prog Retin Eye Res. 2010;29(2):144-68.
7. Damato BE, Coupland SE. Differences in uveal melanomas between men and women from the British Isles. Eye (Lond). 2012;26(2):292-9.
8. Damato EM, Damato BE. Detection and time to treatment of uveal melanoma in the United Kingdom: an evaluation of 2,384 patients. Ophthalmology. 2012;119(8):1582-9.
9. Angi M. Identification of biomarkers of metastatic disease in uveal melanoma using proteomic analyses. Liverpool: University of Liverpool; 2015.
10. A. Armstrong RPC. The Eye and Vision: An Overview. In: Preedy VR, editor. Handbook of Nutrition, Diet and the Eye: Academic Press; 2014. p. 3-9.
11. OMF. Uveal Melanoma Diagnosis. 2013.
12. Rishi P, Shields CL, Khan MA, Patrick K, Shields JA. Headache or eye pain as the presenting feature of uveal melanoma. Ophthalmology. 2013;120(9):1946-7 e2.
13. Amin MB, Greene FL, Edge SB, Compton CC, Gershenwald JE, Brookland RK, et al. The Eighth Edition AJCC Cancer Staging Manual: Continuing to build a bridge from a population-based to a more "personalized" approach to cancer staging. CA Cancer J Clin. 2017;67(2):93-9.
14. Kujala E, Damato B, Coupland SE, Desjardins L, Bechrakis NE, Grange JD, et al. Staging of ciliary body and choroidal melanomas based on anatomic extent. J Clin Oncol. 2013;31(22):2825-31.
15. Yang J, Manson DK, Marr BP, Carvajal RD. Treatment of uveal melanoma: where are we now? Ther Adv Med Oncol. 2018;10:1758834018757175.
16. American Brachytherapy Society - Ophthalmic Oncology Task Force. Electronic address pec, Committee AO. The American Brachytherapy Society consensus guidelines for plaque brachytherapy of uveal melanoma and retinoblastoma. Brachytherapy. 2014;13(1):1-14.
17. Jampol LM, Moy CS, Murray TG, Reynolds SM, Albert DM, Schachat AP, et al. The COMS randomized trial of iodine 125 brachytherapy for choroidal melanoma: IV. Local treatment failure and enucleation in the first 5 years after brachytherapy. COMS report no. 19. Ophthalmology. 2002;109(12):2197-206.
18. Damato B, Kacperek A, Chopra M, Sheen MA, Campbell IR, Errington RD. Proton beam radiotherapy of iris melanoma. Int J Radiat Oncol Biol Phys. 2005;63(1):109-15.
19. Gunduz K, Shields CL, Shields JA, Cater J, Freire JE, Brady LW. Radiation complications and tumor control after plaque radiotherapy of choroidal melanoma with macular involvement. Am J Ophthalmol. 1999;127(5):579-89.
20. Jensen AW, Petersen IA, Kline RW, Stafford SL, Schomberg PJ, Robertson DM. Radiation complications and tumor control after 125I plaque brachytherapy for ocular melanoma. Int J Radiat Oncol Biol Phys. 2005;63(1):101-8.
21. Desjardins L, Lumbroso-Le Rouic L, Levy-Gabriel C, Cassoux N, Dendale R, Mazal A, et al. Treatment of uveal melanoma by accelerated proton beam. Dev Ophthalmol. 2012;49:41-57.
22. Bensoussan E, Thariat J, Maschi C, Delas J, Schouver ED, Herault J, et al. Outcomes After Proton Beam Therapy for Large Choroidal Melanomas in 492 Patients. Am J Ophthalmol. 2016;165:78-87.

23. Brockhurst RJ. Tantalum buttons for localization of malignant melanoma in proton beam therapy. Ophthalmic Surg. 1980;11(5):352.
24. Kim IK, Lane AM, Egan KM, Munzenrider J, Gragoudas ES. Natural history of radiation papillopathy after proton beam irradiation of parapapillary melanoma. Ophthalmology. 2010;117(8):1617-22.
25. Damato B, Patel I, Campbell IR, Mayles HM, Errington RD. Local tumor control after 106Ru brachytherapy of choroidal melanoma. Int J Radiat Oncol Biol Phys. 2005;63(2):385-91.
26. Henderson MA, Shirazi H, Lo SS, Mendonca MS, Fakiris AJ, Witt TC, et al. Stereotactic radiosurgery and fractionated stereotactic radiotherapy in the treatment of uveal melanoma. Technol Cancer Res Treat. 2006;5(4):411-9.
27. Muller K, Naus N, Nowak PJ, Schmitz PI, de Pan C, van Santen CA, et al. Fractionated stereotactic radiotherapy for uveal melanoma, late clinical results. Radiother Oncol. 2012;102(2):219-24.
28. Gunduz K, Bechrakis NE. Exoresection and endoresection for uveal melanoma. Middle East Afr J Ophthalmol. 2010;17(3):210-6.
29. Damato B. Adjunctive plaque radiotherapy after local resection of uveal melanoma. Front Radiat Ther Oncol. 1997;30:123-32.
30. Turcotte S, Bergeron D, Rousseau AP, Mouriaux F. Primary transpupillary thermotherapy for choroidal indeterminate melanocytic lesions. Can J Ophthalmol. 2014;49(5):464-7.
31. Campbell WG, Pejnovic TM. Treatment of amelanotic choroidal melanoma with photodynamic therapy. Retina. 2012;32(7):1356-62.
32. Keunen JE, Journee-de Korver JG, Oosterhuis JA. Transpupillary thermotherapy of choroidal melanoma with or without brachytherapy: a dilemma. Br J Ophthalmol. 1999;83(8):987-8.
33. Mashayekhi A, Shields CL, Rishi P, Atalay HT, Pellegrini M, McLaughlin JP, et al. Primary transpupillary thermotherapy for choroidal melanoma in 391 cases: importance of risk factors in tumor control. Ophthalmology. 2015;122(3):600-9.
34. Damato B. Progress in the management of patients with uveal melanoma. The 2012 Ashton Lecture. Eye (Lond). 2012;26(9):1157-72.
35. Damato B, Coupland SE. A reappraisal of the significance of largest basal diameter of posterior uveal melanoma. Eye (Lond). 2009;23(12):2152-60; quiz 61-2.
36. Shields CL, Kaliki S, Furuta M, Fulco E, Alarcon C, Shields JA. American Joint Committee on Cancer classification of posterior uveal melanoma (tumor size category) predicts prognosis in 7731 patients. Ophthalmology. 2013;120(10):2066-71.
37. McLean IW, Zimmerman LE, Evans RM. Reappraisal of Callender's spindle a type of malignant melanoma of choroid and ciliary body. Am J Ophthalmol. 1978;86(4):557-64.
38. Angi M, Damato B, Kalirai H, Dodson A, Taktak A, Coupland SE. Immunohistochemical assessment of mitotic count in uveal melanoma. Acta Ophthalmol. 2011;89(2):e155-60.
39. Kivela T, Makitie T, Al-Jamal RT, Toivonen P. Microvascular loops and networks in uveal melanoma. Can J Ophthalmol. 2004;39(4):409-21.
40. Dopierala J, Damato BE, Lake SL, Taktak AF, Coupland SE. Genetic heterogeneity in uveal melanoma assessed by multiplex ligation-dependent probe amplification. Invest Ophthalmol Vis Sci. 2010;51(10):4898-905.
41. Prescher G, Bornfeld N, Hirche H, Horsthemke B, Jockel KH, Becher R. Prognostic implications of monosomy 3 in uveal melanoma. Lancet. 1996;347(9010):1222-5.
42. Damato B, Dopierala JA, Coupland SE. Genotypic profiling of 452 choroidal melanomas with multiplex ligation-dependent probe amplification. Clin Cancer Res. 2010;16(24):6083-92.
43. Caines R, Eleuteri A, Kalirai H, Fisher AC, Heimann H, Damato BE, et al. Cluster analysis of multiplex ligation-dependent probe amplification data in choroidal melanoma. Mol Vis. 2015;21:1-11.

44. Kilic E, Naus NC, van Gils W, Klaver CC, van Til ME, Verbiest MM, et al. Concurrent loss of chromosome arm 1p and chromosome 3 predicts a decreased disease-free survival in uveal melanoma patients. Invest Ophthalmol Vis Sci. 2005;46(7):2253-7.
45. Furney SJ, Pedersen M, Gentien D, Dumont AG, Rapinat A, Desjardins L, et al. SF3B1 mutations are associated with alternative splicing in uveal melanoma. Cancer Discov. 2013;3(10):1122-9.
46. Van Raamsdonk CD, Griewank KG, Crosby MB, Garrido MC, Vemula S, Wiesner T, et al. Mutations in GNA11 in uveal melanoma. N Engl J Med. 2010;363(23):2191-9.
47. Jensen DE, Proctor M, Marquis ST, Gardner HP, Ha SI, Chodosh LA, et al. BAP1: a novel ubiquitin hydrolase which binds to the BRCA1 RING finger and enhances BRCA1-mediated cell growth suppression. Oncogene. 1998;16(9):1097-112.
48. Yu H, Mashtalir N, Daou S, Hammond-Martel I, Ross J, Sui G, et al. The ubiquitin carboxyl hydrolase BAP1 forms a ternary complex with YY1 and HCF-1 and is a critical regulator of gene expression. Mol Cell Biol. 2010;30(21):5071-85.
49. Kalirai H, Dodson A, Faqir S, Damato BE, Coupland SE. Lack of BAP1 protein expression in uveal melanoma is associated with increased metastatic risk and has utility in routine prognostic testing. Br J Cancer. 2014;111(7):1373-80.
50. Farquhar N, Thornton S, Coupland SE, Coulson JM, Sacco JJ, Krishna Y, et al. Patterns of BAP1 protein expression provide insights into prognostic significance and the biology of uveal melanoma. J Pathol Clin Res. 2018;4(1):26-38.
51. Koopmans AE, Verdijk RM, Brouwer RW, van den Bosch TP, van den Berg MM, Vaarwater J, et al. Clinical significance of immunohistochemistry for detection of BAP1 mutations in uveal melanoma. Mod Pathol. 2014;27(10):1321-30.
52. van de Nes JA, Nelles J, Kreis S, Metz CH, Hager T, Lohmann DR, et al. Comparing the Prognostic Value of BAP1 Mutation Pattern, Chromosome 3 Status, and BAP1 Immunohistochemistry in Uveal Melanoma. Am J Surg Pathol. 2016;40(6):796-805.
53. Robertson AG, Shih J, Yau C, Gibb EA, Oba J, Mungall KL, et al. Integrative Analysis Identifies Four Molecular and Clinical Subsets in Uveal Melanoma. Cancer Cell. 2017;32(2):204-20 e15.
54. Ardjomand N, Komericki P, Langmann G, Mattes D, Moray M, Scarpatetti M, et al. Lymph node metastases arising from uveal melanoma. Wien Klin Wochenschr. 2005;117(11-12):433-5.
55. Lorigan JG, Wallace S, Mavligit GM. The prevalence and location of metastases from ocular melanoma: imaging study in 110 patients. AJR Am J Roentgenol. 1991;157(6):1279-81.
56. Paget S. The distribution of secondary growths in cancer of the breast. 1889. Cancer Metastasis Rev. 1989;8(2):98-101.
57. Eskelin S, Pyrhonen S, Summanen P, Hahka-Kemppinen M, Kivela T. Tumor doubling times in metastatic malignant melanoma of the uvea: tumor progression before and after treatment. Ophthalmology. 2000;107(8):1443-9.
58. Blanco PL, Lim LA, Miyamoto C, Burnier MN. Uveal melanoma dormancy: an acceptable clinical endpoint? Melanoma Res. 2012;22(5):334-40.
59. Cerbone L, Van Ginderdeuren R, Van den Oord J, Fieuws S, Spileers W, Van Eenoo L, et al. Clinical presentation, pathological features and natural course of metastatic uveal melanoma, an orphan and commonly fatal disease. Oncology. 2014;86(3):185-9.
60. Hicks C, Foss AJ, Hungerford JL. Predictive power of screening tests for metastasis in uveal melanoma. Eye (Lond). 1998;12 (Pt 6):945-8.
61. Marshall E, Romaniuk C, Ghaneh P, Wong H, McKay M, Chopra M, et al. MRI in the detection of hepatic metastases from high-risk uveal melanoma: a prospective study in 188 patients. Br J Ophthalmol. 2013;97(2):159-63.
62. Diener-West M, Reynolds SM, Agugliaro DJ, Caldwell R, Cumming K, Earle JD, et al. Screening for metastasis from choroidal melanoma: the Collaborative Ocular Melanoma Study Group Report 23. J Clin Oncol. 2004;22(12):2438-44.

63. Belmar-Lopez C, Mancheno-Corvo P, Saornil MA, Baril P, Vassaux G, Quintanilla M, et al. Uveal vs. cutaneous melanoma. Origins and causes of the differences. Clin Transl Oncol. 2008;10(3):137-42.
64. Thomas AJ, Erickson CA. The making of a melanocyte: the specification of melanoblasts from the neural crest. Pigment Cell Melanoma Res. 2008;21(6):598-610.
65. Coupland SE, Damato BE. Molecular analysis of uveal melanoma. Ophthalmology. 2013;120(7):e50.
66. Simoes-Costa M, Bronner ME. Establishing neural crest identity: a gene regulatory recipe. Development. 2015;142(2):242-57.
67. Sauka-Spengler T, Bronner-Fraser M. A gene regulatory network orchestrates neural crest formation. Nat Rev Mol Cell Biol. 2008;9(7):557-68.
68. Mort RL, Jackson IJ, Patton EE. The melanocyte lineage in development and disease. Development. 2015;142(4):620-32.
69. Cheli Y, Ohanna M, Ballotti R, Bertolotto C. Fifteen-year quest for microphthalmia-associated transcription factor target genes. Pigment Cell Melanoma Res. 2010;23(1):27-40.
70. Watanabe K, Takeda K, Yasumoto K, Udono T, Saito H, Ikeda K, et al. Identification of a distal enhancer for the melanocyte-specific promoter of the MITF gene. Pigment Cell Res. 2002;15(3):201-11.
71. Clarke MF, Fuller M. Stem cells and cancer: two faces of eve. Cell. 2006;124(6):1111-5.
72. Lapidot T, Sirard C, Vormoor J, Murdoch B, Hoang T, Caceres-Cortes J, et al. A cell initiating human acute myeloid leukaemia after transplantation into SCID mice. Nature. 1994;367(6464):645-8.
73. Morrison SJ, Weissman IL. The long-term repopulating subset of hematopoietic stem cells is deterministic and isolatable by phenotype. Immunity. 1994;1(8):661-73.
74. Shackleton M. Normal stem cells and cancer stem cells: similar and different. Semin Cancer Biol. 2010;20(2):85-92.
75. Pattabiraman DR, Weinberg RA. Tackling the cancer stem cells - what challenges do they pose? Nat Rev Drug Discov. 2014;13(7):497-512.
76. Clarke MF, Dick JE, Dirks PB, Eaves CJ, Jamieson CH, Jones DL, et al. Cancer stem cells--perspectives on current status and future directions: AACR Workshop on cancer stem cells. Cancer Res. 2006;66(19):9339-44.
77. Qureshi-Baig K, Ullmann P, Haan S, Letellier E. Tumor-Initiating Cells: a criTICal review of isolation approaches and new challenges in targeting strategies. Mol Cancer. 2017;16(1):40.
78. Hu DN, McCormick SA, Ritch R, Pelton-Henrion K. Studies of human uveal melanocytes in vitro: isolation, purification and cultivation of human uveal melanocytes. Invest Ophthalmol Vis Sci. 1993;34(7):2210-9.
79. Angi M, Versluis M, Kalirai H. Culturing Uveal Melanoma Cells. Ocul Oncol Pathol. 2015;1(3):126-32.
80. Zhao Q, Guo X, Nash GB, Stone PC, Hilkens J, Rhodes JM, et al. Circulating galectin-3 promotes metastasis by modifying MUC1 localization on cancer cell surface. Cancer Res. 2009;69(17):6799-806.
81. Brychtova S, Fiuraskova M, Hlobilkova A, Brychta T, Hirnak J. Nestin expression in cutaneous melanomas and melanocytic nevi. J Cutan Pathol. 2007;34(5):370-5.
82. Djirackor L, Shakir D, Kalirai H, Petrovski G, Coupland SE. Nestin expression in primary and metastatic uveal melanoma - possible biomarker for high-risk uveal melanoma. Acta Ophthalmol. 2018.
83. Yilmaz G, Akyol G, Cakir A, Ilhan M. Investigation of diagnostic utility and expression profiles of stem cell markers (CD133 and CD90) in hepatocellular carcinoma, small cell dysplasia, and cirrhosis. Pathol Res Pract. 2014;210(7):419-25.
84. Inocencio J, Frenster JD, Placantonakis DG. Isolation of Glioblastoma Stem Cells with Flow Cytometry. Methods Mol Biol. 2018;1741:71-9.

85. Nagata H, Ishihara S, Kishikawa J, Sonoda H, Murono K, Emoto S, et al. CD133 expression predicts post-operative recurrence in patients with colon cancer with peritoneal metastasis. Int J Oncol. 2018;52(3):721-32.
86. Johnson JP, Rothbacher U, Sers C. The progression associated antigen MUC18: a unique member of the immunoglobulin supergene family. Melanoma Res. 1993;3(5):337-40.
87. Lei X, Guan CW, Song Y, Wang H. The multifaceted role of CD146/MCAM in the promotion of melanoma progression. Cancer Cell Int. 2015;15(1):3.
88. Lunter PC, van Kilsdonk JW, van Beek H, Cornelissen IM, Bergers M, Willems PH, et al. Activated leukocyte cell adhesion molecule (ALCAM/CD166/MEMD), a novel actor in invasive growth, controls matrix metalloproteinase activity. Cancer Res. 2005;65(19):8801-8.
89. van Kempen LC, van den Oord JJ, van Muijen GN, Weidle UH, Bloemers HP, Swart GW. Activated leukocyte cell adhesion molecule/CD166, a marker of tumor progression in primary malignant melanoma of the skin. Am J Pathol. 2000;156(3):769-74.
90. Kulesa PM, Morrison JA, Bailey CM. The neural crest and cancer: a developmental spin on melanoma. Cells Tissues Organs. 2013;198(1):12-21.
91. Hou L, Pavan WJ. Transcriptional and signaling regulation in neural crest stem cell-derived melanocyte development: do all roads lead to Mitf? Cell Res. 2008;18(12):1163-76.
92. Mouriaux F, Kherrouche Z, Maurage CA, Demailly FX, Labalette P, Saule S. Expression of the c-kit receptor in choroidal melanomas. Melanoma Res. 2003;13(2):161-6.
93. Calipel A, Landreville S, De La Fouchardiere A, Mascarelli F, Rivoire M, Penel N, et al. Mechanisms of resistance to imatinib mesylate in KIT-positive metastatic uveal melanoma. Clin Exp Metastasis. 2014;31(5):553-64.
94. Piras F, Perra MT, Murtas D, Minerba L, Floris C, Maxia C, et al. The stem cell marker nestin predicts poor prognosis in human melanoma. Oncol Rep. 2010;23(1):17-24.
95. Klein WM, Wu BP, Zhao S, Wu H, Klein-Szanto AJ, Tahan SR. Increased expression of stem cell markers in malignant melanoma. Mod Pathol. 2007;20(1):102-7.
96. Donizy P, Zietek M, Halon A, Leskiewicz M, Kozyra C, Matkowski R. Prognostic significance of ALCAM (CD166/MEMD) expression in cutaneous melanoma patients. Diagn Pathol. 2015;10:86.
97. Lai K, Sharma V, Jager MJ, Conway RM, Madigan MC. Expression and distribution of MUC18 in human uveal melanoma. Virchows Arch. 2007;451(5):967-76.
98. Rao C, Bui T, Connelly M, Doyle G, Karydis I, Middleton MR, et al. Circulating melanoma cells and survival in metastatic melanoma. Int J Oncol. 2011;38(3):755-60.
99. Roland CL, Ross MI, Hall CS, Laubacher B, Upshaw J, Anderson AE, et al. Detection of circulating melanoma cells in the blood of melanoma patients: a preliminary study. Melanoma Res. 2015;25(4):335-41.
100. Paoli P, Giannoni E, Chiarugi P. Anoikis molecular pathways and its role in cancer progression. Biochim Biophys Acta. 2013;1833(12):3481-98.
101. Frisch SM, Schaller M, Cieply B. Mechanisms that link the oncogenic epithelial-mesenchymal transition to suppression of anoikis. J Cell Sci. 2013;126(Pt 1):21-9.
102. Kim SY, Hong SH, Basse PH, Wu C, Bartlett DL, Kwon YT, et al. Cancer Stem Cells Protect Non-Stem Cells From Anoikis: Bystander Effects. J Cell Biochem. 2016;117(10):2289-301.
103. Civenni G, Walter A, Kobert N, Mihic-Probst D, Zipser M, Belloni B, et al. Human CD271-positive melanoma stem cells associated with metastasis establish tumor heterogeneity and long-term growth. Cancer Res. 2011;71(8):3098-109.
104. Thill M, Berna MJ, Grierson R, Reinhart I, Voelkel T, Piechaczek C, et al. Expression of CD133 and other putative stem cell markers in uveal melanoma. Melanoma Res. 2011;21(5):405-16.
105. Levesque MC, Heinly CS, Whichard LP, Patel DD. Cytokine-regulated expression of activated leukocyte cell adhesion molecule (CD166) on monocyte-lineage cells and in rheumatoid arthritis synovium. Arthritis Rheum. 1998;41(12):2221-9.
106. Ohneda O, Ohneda K, Arai F, Lee J, Miyamoto T, Fukushima Y, et al. ALCAM (CD166): its role in hematopoietic and endothelial development. Blood. 2001;98(7):2134-42.

107. Weiner JA, Koo SJ, Nicolas S, Fraboulet S, Pfaff SL, Pourquie O, et al. Axon fasciculation defects and retinal dysplasias in mice lacking the immunoglobulin superfamily adhesion molecule BEN/ALCAM/SC1. Mol Cell Neurosci. 2004;27(1):59-69.
108. Nagymihaly R, Vereb Z, Albert R, Sidney L, Dua H, Hopkinson A, et al. Cultivation and characterisation of the surface markers and carbohydrate profile of human corneal endothelial cells. Clin Exp Ophthalmol. 2017;45(5):509-19.
109. Dorfmueller S, Tan HC, Ngoh ZX, Toh KY, Peh G, Ang HP, et al. Isolation of a recombinant antibody specific for a surface marker of the corneal endothelium by phage display. Sci Rep. 2016;6:21661.
110. Burns FR, von Kannen S, Guy L, Raper JA, Kamholz J, Chang S. DM-GRASP, a novel immunoglobulin superfamily axonal surface protein that supports neurite extension. Neuron. 1991;7(2):209-20.
111. Tanaka H, Matsui T, Agata A, Tomura M, Kubota I, McFarland KC, et al. Molecular cloning and expression of a novel adhesion molecule, SC1. Neuron. 1991;7(4):535-45.
112. Onken MD, Worley LA, Ehlers JP, Harbour JW. Gene expression profiling in uveal melanoma reveals two molecular classes and predicts metastatic death. Cancer Res. 2004;64(20):7205-9.
113. Chang SH, Worley LA, Onken MD, Harbour JW. Prognostic biomarkers in uveal melanoma: evidence for a stem cell-like phenotype associated with metastasis. Melanoma Res. 2008;18(3):191-200.
114. Krupkova O, Jr., Loja T, Zambo I, Veselska R. Nestin expression in human tumors and tumor cell lines. Neoplasma. 2010;57(4):291-8.
115. Singh SK, Clarke ID, Terasaki M, Bonn VE, Hawkins C, Squire J, et al. Identification of a cancer stem cell in human brain tumors. Cancer Res. 2003;63(18):5821-8.
116. Veselska R, Hermanova M, Loja T, Chlapek P, Zambo I, Vesely K, et al. Nestin expression in osteosarcomas and derivation of nestin/CD133 positive osteosarcoma cell lines. BMC Cancer. 2008;8:300.
117. Sabet MN, Rakhshan A, Erfani E, Madjd Z. Co-expression of putative cancer stem cell markers, CD133 and Nestin, in skin tumors. Asian Pac J Cancer Prev. 2014;15(19):8161-9.
118. Laurent C, Valet F, Planque N, Silveri L, Maacha S, Anezo O, et al. High PTP4A3 phosphatase expression correlates with metastatic risk in uveal melanoma patients. Cancer Res. 2011;71(3):666-74.
119. Kalirai H, Damato BE, Coupland SE. Uveal melanoma cell lines contain stem-like cells that self-renew, produce differentiated progeny, and survive chemotherapy. Invest Ophthalmol Vis Sci. 2011;52(11):8458-66.
120. Fusi A, Reichelt U, Busse A, Ochsenreither S, Rietz A, Maisel M, et al. Expression of the stem cell markers nestin and CD133 on circulating melanoma cells. J Invest Dermatol. 2011;131(2):487-94.
121. Fusi A, Ochsenreither S, Busse A, Rietz A, Keilholz U. Expression of the stem cell marker nestin in peripheral blood of patients with melanoma. Br J Dermatol. 2010;163(1):107-14.
122. Barak V, Frenkel S, Valyi-Nagy K, Leach L, Apushkin MA, Lin AY, et al. Using the direct-injection model of early uveal melanoma hepatic metastasis to identify TPS as a potentially useful serum biomarker. Invest Ophthalmol Vis Sci. 2007;48(10):4399-402.
123. Suesskind D, Schatz A, Schnichels S, Coupland SE, Lake SL, Wissinger B, et al. GDF-15: a novel serum marker for metastases in uveal melanoma patients. Graefes Arch Clin Exp Ophthalmol. 2012;250(6):887-95.
124. Akiyama M, Matsuda Y, Ishiwata T, Naito Z, Kawana S. Inhibition of the stem cell marker nestin reduces tumor growth and invasion of malignant melanoma. J Invest Dermatol. 2013;133(5):1384-7.
125. Ishiwata T, Teduka K, Yamamoto T, Kawahara K, Matsuda Y, Naito Z. Neuroepithelial stem cell marker nestin regulates the migration, invasion and growth of human gliomas. Oncol Rep. 2011;26(1):91-9.

126. Matsuda Y, Kure S, Ishiwata T. Nestin and other putative cancer stem cell markers in pancreatic cancer. Med Mol Morphol. 2012;45(2):59-65.